

國立交通大學

電信工程學系碩士班

碩士論文

利用子符號多項式內插實現 OFDM 通道估計  
OFDM Channel Estimation Based on Sub-symbol  
Polynomial Interpolation

The logo of National Central University (NCU) is a circular emblem. It features a central shield with a book and a torch, surrounded by a gear-like border. The year '1896' is inscribed at the bottom of the shield. The entire emblem is rendered in a light blue color.

研究生：吳柏學

指導教授：謝世福 博士

中華民國九十三年七月

利用子符號多項式內插實現 OFDM 通道估計

**OFDM Channel Estimation Based on  
Sub-symbol Polynomial Interpolation**

研 究 生：吳柏學

Student： B. X. Wu

指導教授：謝世福 博士

Advisor： Dr. S. F. Hsieh



A Thesis

Submitted to Department of Communication Engineering  
College of Electrical Engineering and Computer Science  
National Chiao Tung University

In Partial Fulfillment of the Requirements

For the Degree of  
Master of Science

In

Electrical Engineering

July, 2004

Hsinchu, Taiwan, Republic of China

中華民國九十三年七月


# 利用子符號多項式內插實現 OFDM 通道估計

學生:吳柏學

指導教授:謝世福

國立交通大學電信工程學系碩士班

## 摘要



在 OFDM 系統的通道估計上,通常藉由訓練訊號 (Training signal) 的輔助來找出通道響應。但考慮到通道的時變性,使用訓練訊號求得的通道響應,並不能代表資料訊號(Data signal)的通道狀況。在快速衰減的通道下,我們提出子符號多項式內插方法配合最強路徑選取(most significant taps)演算法來內插出資料訊號的通道響應。在子符號多項式內插上,將均方誤差分成模型誤差跟雜訊誤差,討論不同系統參數包括都卜勒頻率,訓練率(Training rate)和多項式階數。我們會使用一個已知統計特性的通道模型檢查推導出來的誤差與模擬誤差是否配合。最後拿子符號內插法比較其他現有的多項式內插方法,直接判斷演算法(Decision direct algorithm)與線性內插方法,子訊號內插法方法會有最好的表現。

# OFDM Channel Estimation Based on Sub-Symbol Polynomial Interpolation


Student: B. X. Wu

Advisor: S. F. Hsieh

Department of Communication Engineering

National Chiao Tung University

## Abstract



In OFDM channel estimation, we usually utilize training signals. In case of a time varying channel environment, the channel responses, estimated during training period, can't represent the channel during data transmission. In such fast fading channel, we propose the sub-symbol polynomial interpolation algorithm that retains most significant taps algorithm to interpolate channel responses in data position. We derives its mean square error (MSE) that includes both model and noise errors. We verify the MSE performances of the derived results and the simulation results by using a time varying channel, whose statistics are known. The proposed sub-symbol polynomial interpolation that is the most effective in the fast fading channel, compared with the existing polynomial interpolation, the decision direct algorithm, and the linear interpolation.

# Acknowledgements

Firstly, I would like to express my sincere gratitude to my advisor, Dr. S. F. Hsieh, for his enthusiastic guidance and great patient in my research. Secondly, I also appreciate all my lab-mates very much for their help. Secondly, I would like to show my sincere thanks to my family for their encouragement and love. Finally, I want to show my gratitude to B. C. Ho, because she arouses my potential in many ways.



# Contents

<b>1. Introduction</b>	<b>1</b>
<b>2. Time Domain Approach for OFDM Channel Estimation</b>	<b>6</b>
2.1 System description.....	7
2.2 FPTA channel estimation .....	9
2.2.1 FPTA channel estimation algorithm.....	10
2.2.2 Analysis of channel estimation error of FPTA... ..	11
2.3 MST channel estimation .....	12
2.3.1 MST channel estimation algorithm.....	13
2.3.2 Analysis of channel estimation error of MST.....	14
2.4 FPTA with LMMSE channel estimation method.....	16
2.4.1 LMMSE channel estimation algorithm.....	17

### **3. Time Varying Channel Tracking** **19**

3.1	Time varying channel model.....	20
3.1.1	DGUS channel model.....	20
3.1.2	Statistic properties of DGUS channel.....	22
3.2	The FPTA method and The MST method in time varying channel.....	24
3.2.1	FPTA and MST with decision direct algorithm.....	25
3.2.1	FPTA and MST with linear interpolation algorithm.....	26
3.3	Sub-symbol polynomial interpolation.....	28
3.3.1	Sub-symbol polynomial interpolation algorithm.....	29
3.3.2	The MST algorithm for sub-symbol polynomial interpolation.....	32
3.3.3	Analysis of channel estimation error of sub-symbol polynomial interpolation.....	33
3.4	Polynomial interpolation of channel in time-frequency domain.....	36
3.4.1	Polynomial interpolation algorithm in time-frequency domain.....	37
3.4.2	The comparison between sub-symbol polynomial interpolation and time-frequency domain interpolation.....	40

### **4. Computer Simulations** **42**

4.1	Simulation parameters.....	42
-----	----------------------------	----

4.2 Comparison between FPTA, MST and LMMSE	
in time invariant channel.....	43
4.3 Comparison between channel estimation methods	
in time varying channel.....	46
4.4 Properties of sub-symbol polynomial interpolation.....	49
4.4.1 Comparison of different Doppler frequency.....	50
4.4.2 Comparison of different training rate.....	51
4.4.3 Comparison of different polynomial order.....	52
4.4.4 Comparison of different Channel.....	54

## 5. Conclusions



56



# List of Figure

2.1	OFDM system block diagram, transmitter and receiver.....	7
2.2	Data grid in time-frequency plane of an OFDM signals.....	8
3.1	Block of One-tap Recursive Least Square filter.....	25
3.2	Illustration of linear interpolation.....	26
3.3	Channel tracking by sub-symbol polynomial interpolation.....	30
3.4	Data grid in the time-frequency plane of OFDM signals.....	38
3.5	Channel responses distribute in time-frequency plane.....	41
4.1	Channel estimation mean square error (MSE) in TI Channel-A.....	45
4.2	BER performance with different channel estimation methods in TI Channel-A.....	46
4.3	Channel estimation MSE performance with different threshold selections in TI Channel-A.....	46
4.4	BER performance with different threshold selections in TI Channel-A.....	47
4.5	MSE performance with different channel estimation methods in Doppler frequency 75Hz environment.....	48
4.6	BER performance with different channel estimation methods in Doppler frequency 75Hz environment.....	49

4.7	BER performance with different taps selection of Combing MST and sub-symbol polynomial interpolation.....	50
4.8	Channel estimation MSE with different Doppler frequencies in TV Channel-A.....	51
4.9	Channel estimation MSE with different training rates in TV Channel-A....	53
4.10	Channel estimation MSE with different polynomial order in TV Channel-A54.....	54
4.11	Channel estimation MSE in TV Channel-A and TV Channel-B and $f_d = 150\text{Hz}, 200\text{Hz}$ .....	55



# Chapter 1

## Introduction

Orthogonal frequency division multiplexing (OFDM) has recently become popular due to its desirable properties such as its robustness to intersymbol interference (ISI) and impulse noise, its high data rate transmission capability with high bandwidth efficiency, and its feasibility in application of adaptive modulation and power allocation across the subcarriers according to the channel conditions [1]-[3]. It has been adapted in many applications such as ADSL (Asymmetric Digital Subscriber Line) [4], broadcasting Services such as European DAB (Digital Audio Broadcasting) [5], DVB-T (Terrestrial Integrated Services Digital Broadcasting) [6] and multimedia wireless services such as Japanese MMAC (Multimedia Mobile Access Communication) [7].

The independence among subcarriers simplifies the design of the equalizer and provides an easy method for data recovery. Since the channel information is required in equalization. Channel estimation plays an important role in OFDM system design. Channel estimation is a challenging problem in wireless communications. Because of the mobility of the transmitter, the receiver, or the scattering objects, the channel response can change rapidly with time.

In typical OFDM systems, some part of the transmitted signal is known. In one approach, the transmitter periodically provides known training sequences, which can be used for channel estimation. In a second approach, the pilot channels are provided for channel estimation. This approach is related to the pilot tone approach [8]-[10]. The pilot channels are stronger in power than the information channels.

When there are sufficiently strong pilot channels or sufficient pilot sequence, the channel can be tracked by filtering channel measurements obtained from the pilot information. The filter smoothes the noisy measurements over time and works best when the channel estimate is based on future as well as past channel measurements. Specifically, for a given filter, channel estimation performance depends on the pilot information, fading channel characteristics, and noise level. Pilot information, in term of how much energy and how often it is available, is a tradeoff between minimizing overhead and optimizing channel estimation performance. For example, with pilot symbols, how often symbols must be sent depends on how rapidly the channel is changing.

In channel estimation based on training symbol for time varying channel, some methods need information of statistics of channel [11]-[12]. Channel estimation based on statistics of channel is more complex, but its performance is usually better, depending on the accuracy of the Wiener filter quantities. Channel estimation based on correlation of channel requires knowledge of the statistics of the fading process and the statistics of the measurement noise process. The fading process statistics can be related to parameters of a channel model, such as Doppler spread and average channel coefficient power. Such information is usually unknown. There are many ways to find the statistics of fading process and noise process, but they increase system complexity. The statistics of channel also change with time. The change of

statistics of channel will cause mismatch problem [11]. The performance will be degraded. In order to decrease complexity of channel estimation, we focus on the channel estimation methods without using statistics of channel. One of the simplest forms of channel estimation using pilot symbols is the linear interpolation [13]. With linear interpolation, the channel estimate at a certain time period is a linear combination of the two nearest channel measurements. Linear interpolation can be viewed as applying a filter with symbol-spaced taps to the channel measurements, which contain zeros at the unknown data symbol points. It may get worse channel estimation in cases of high Doppler shift and long distance between training sequence.

We use the polynomial interpolation in this thesis. Compared to the linear interpolation with polynomial interpolation, the polynomial interpolation is more accurate to model a time varying channel. It may have higher complexity than the linear interpolation, but it saves large complexity than the channel estimation based on statistics of channel. The polynomial interpolation can be done in the time domain, in the frequency domain, and in both time and frequency domain [14]-[16]. Some OFDM systems have many subcarriers. There will be a long symbol duration in this system. Channel will is likely to change within one OFDM symbol. We define this rapid change of channel as fast fading channel. The sub-symbol polynomial is proposed for the fast fading channel. The estimation error of sub-symbol is divided into two parts. One is noise error, caused from the noise of the system. The other is model error, which is the difference between real channel impulse and polynomial model. Because the model error is depends on the statistics of channel, we use a time varying channel model in Section 3.1. The statistics of channel will be derived and utilized to check performance of model error. Compared to an existing

time-frequency polynomial interpolation [14] with our proposed sub-symbol method, the latter performs better for two reasons. One is the time-frequency polynomial interpolation operated on slow fading channel. It is not suitable to estimate a fast fading channel. The other reason is that the time-frequency polynomial interpolates channel in frequency domain. The channel changes more rapidly in the frequency domain than in the time domain. Interpolation in the frequency domain incurs a larger model error than interpolation in the time domain. In incorporating the MST method in [17], the sub-symbol polynomial interpolation only needs to interpolate specific delay taps. It saves more computation than the polynomial interpolation in frequency domain.

Chapter 2 will discuss the channel estimation methods for time invariant channel. The frequency pilot time averaging [17] method will be introduced first. Then the most significant taps [17] will be introduced to improve channel estimation in time domain. Another improvement of FPTA method, linear minimum mean square [18], is also introduced in Chapter 2. The LMMSE method is based on statistics of channel. In simulation results, we can find that the performance of LMMSE is close to the performance of MST. The implementation of MST is easier than LMMSE. MST seems a better channel estimation method than LMMSE. But MST has a problem of selecting proper number of taps. When the numbers of selected taps are less than real numbers of channel taps, Error floor will occur. We also derive the MSE (mean square error) of this error floor in Chapter 2. The channel in Chapter 2 is considered stationary between two training symbols and equal to the channel of previous training symbol. The channel estimation in one training symbol can be used to recover data.

In Chapter 3, we consider the time varying channel. The channel estimation

method for time varying channel based on training symbol will be introduced. The channel estimation in training symbol will be obtained with FPTA or MST. Then we introduce decision directed algorithm [19], linear interpolation, and proposed sub-symbol polynomial interpolation which is used in fast fading channel. We derived the MSE of channel estimation for sub-symbol polynomial interpolation method. Its MSE is divided into the noise error and model error. We investigate the sensitivity of the noise error and the model error to different system parameters, including the Doppler frequency, the training rate, the polynomial order and two channel models. We also compare the proposed method with an existing polynomial interpolation in Chapter 3. The simulation results are shown in Chapter 4. In Chapter 5, the conclusion is given.



# Chapter2

## Channel estimation in time invariant channel

In this chapter, we will introduce several channel estimation method based on training symbols. The channel in this chapter is time invariant. The channel can be estimated by using training symbol. The estimated channel can be used to recover data because the channel is time invariant. In Section 2.1, The OFDM configuration is displayed. Because Cyclic Prefix is used in the OFDM system, a simple one-tap equalizer achieves data recovery easily. Then frequency pilot time averaging (FPTA) channel estimation method [17] and its performance are introduced in Section 2.2. The most significant taps (MST) channel estimation method [17] which can improve frequency time domain averaging method [17] is introduced in Section 2.3. The missing tap problem will cause error floor in the performance of MST algorithm. The degradation is also derived in this section. Finally, the linear minimum mean square (LMMSE) channel estimation method [18] is introduced in Section 2.4. The LMMSE channel estimation is also based on the FPTA method. The channel statistics and noise process must be known in the LMMSE method. It is more complex than the MST method.



## 2.1 System model

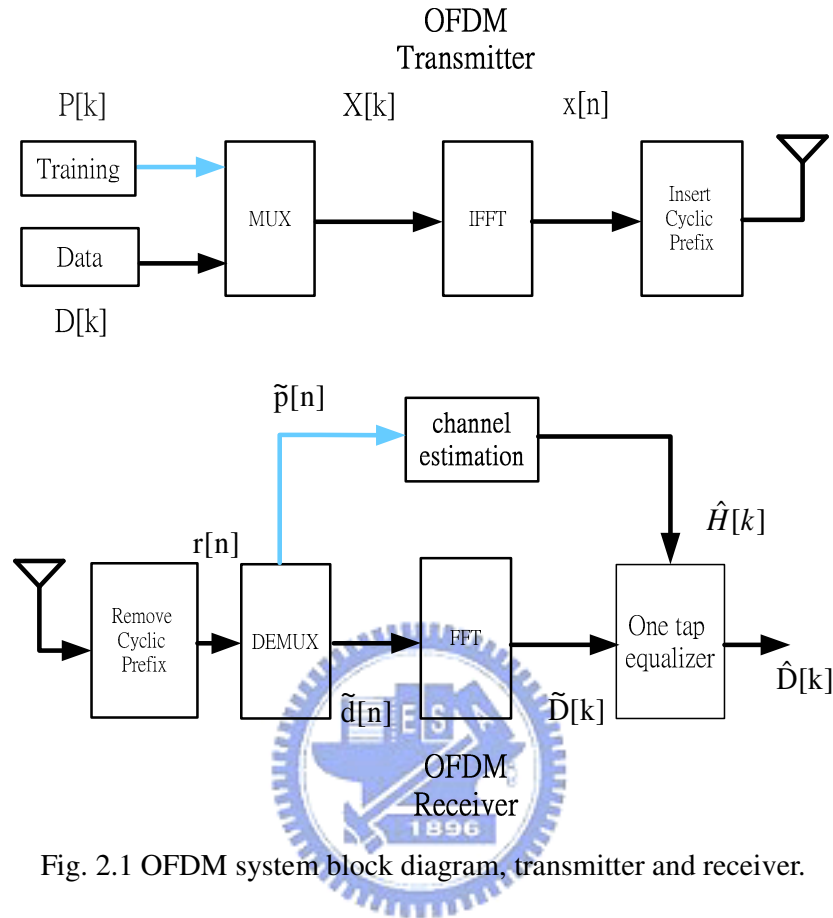


Fig. 2.1 OFDM system block diagram, transmitter and receiver.

In typical OFDM systems as shown in Fig. 2.1, some part of the transmitted signal is training symbol, the transmitter periodically provides known training symbol,  $X[k]$  are called frequency domain signals. The frequency domain signals pass the Inverse Fast Fourier Block, then we get the time domain signals  $x[n]$ . In order to mitigate ISI effect and keep orthogonal property of subcarriers, The Cyclic Prefix (CP) is added before time domain signal. The time domain signals with CP are transmitted in mobile wireless environment. In the receiver side, we remove CP first. Then the received training signals are picked for channel estimation. Suppose the pilot tones  $P[k]$  are located in a time-frequency plane in Figure 2.1. The training symbols are multiplexed with data symbols in all OFDM symbols at a training rate  $P_r$  (ratio

of number of training symbols to number of total symbols). The number of all subcarrier is  $N$  and  $k$  is subcarrier index. The transmitted training signal in discrete-time domain, excluding CP, can be expressed as

$$p[n] = IFFT_N\{P[k]\} \quad (2.1)$$

where  $IFFT_N\{\}$  is an  $N$ -point inverse Fast Fourier transform of an OFDM symbol and  $n$  is the time-domain index,  $n = 0, 1, \dots, N - 1$ . Suppose the wireless channel has a discrete-time impulse response given by

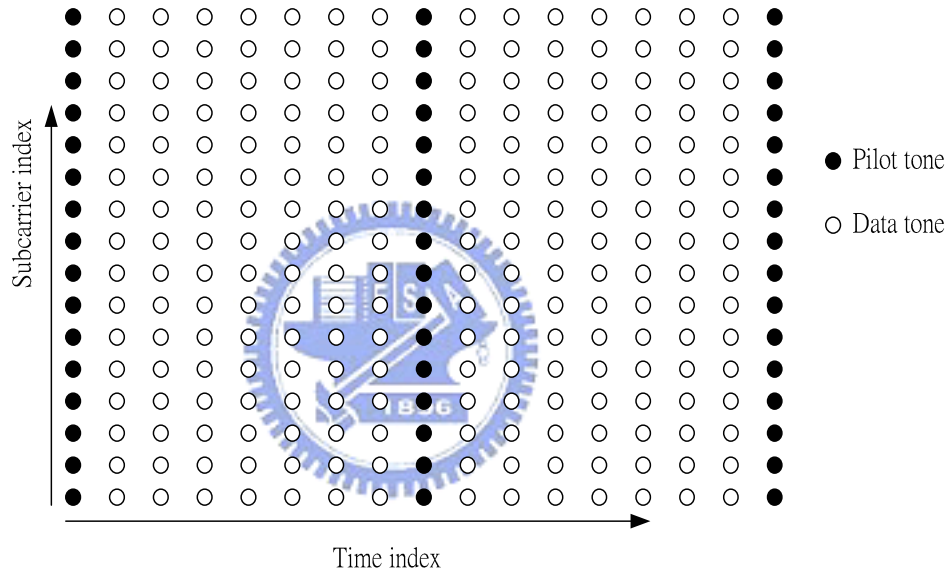


Fig. 2.2 Data grid in time-frequency plane of an OFDM signals

$$h[n] = \sum_{l=0}^{L-1} a_l \delta[n - \tau_l] \quad (2.2)$$

where  $a_l$  is called delay coefficient,  $\tau_l$  is the discrete propagation delay,  $L$  is the number of multipaths. In general, the delay coefficient is uncorrelated between different propagation delay paths. This property will be utilized in LMMSE channel estimation method later in this chapter. After passing through a multipath wireless channel, the time domain received samples of an OFDM symbol, if appropriate cyclic

prefix guard samples are used, is given by

$$r[n] = p[n] \otimes h[n] + w[n] \quad (2.3)$$

where  $\otimes$  represents  $N$ -point circular convolution,  $w[n]$  are independent and identically distributed (iid) AWGN samples with zero mean and variance of  $\sigma_w^2$ . Assuming perfect synchronization, the FFT output frequency-domain subcarrier symbols can be expressed as

$$\begin{aligned} R[k] &= FFT_N\{r[n]\} \\ &= H[k]P[k] + W[k] \end{aligned} \quad (2.4)$$

where  $W[k]$  is Fast Fourier transform of  $w[n]$ . Then the channel frequency response at the pilot tones can be estimated by

$$\hat{H}[k] = \frac{R[k]}{P[k]} = H[k] + \frac{W[k]}{P[k]} \quad (2.5)$$

where  $k$  is the subcarrier index of pilot tones. This rough channel estimation is called LS (least square) estimation [17]. If pilot tones don't occupy all subcarriers, some pilots are zero in the training symbol. The channel responses at those zero tones can be obtained by interpolation.

## 2.2 FPTA channel estimation

A training symbol can be regarded as several time slots, with each time slot having a pilot. In a slow fading channel or time invariant channel assumption, the impulse response of each time slot is identical. A method can obtain the channel response in the time domain by averaging these time slots. This method is referred to as the Frequency Domain Time Average (FPTA) [17] technique.

## 2.2.1 FPTA channel estimation algorithm

In FPTA approach, pilot tones are multiplexed with data at a pilot ratio of  $1/K$  in frequency domain. The frequency domain pilot symbol can be expressed as

$$P[k] = \sum_{m=0}^{M-1} A \delta[k - mK] \quad (2.6)$$

where  $A$  is the pilot amplitude,  $k = 0, 1, \dots, N-1$  and  $M = N/K$  is an integer.

The corresponding time domain samples contain  $K$  identical parts and are given by

$$p[n] = \text{IFFT}\{P[k]\} = \sum_{m=0}^{K-1} \frac{A}{K} \delta[n - mM] \quad (2.7)$$

where  $n = 0, 1, \dots, N-1$ . The time domain received sample vector of a training symbol can be given by

$$\mathbf{r} = \mathbf{p}' + \mathbf{w} \quad (2.8)$$

where  $\mathbf{r} = [r_0, r_1, \dots, r_{K-1}]$ , with  $\mathbf{r}_i = [r_i[0], r_i[1], \dots, r_i[M-1]]$ ,

$\mathbf{w} = [w[0], w[1], \dots, w[N-1]]$ ,  $\mathbf{p}'$  is circular convolution of pilot signal and channel impulse response and can be expressed as  $\mathbf{p}' = [\mathbf{p}_0', \mathbf{p}_1', \dots, \mathbf{p}_{K-1}']$  with

$\mathbf{p}_i' = [p_i'[0], p_i'[1], \dots, p_i'[M-1]]$ . If the maximum channel delay spread is shorter

than the length of an time domain identical part,  $\mathbf{p}_i' = \mathbf{p}_j'$ , for  $i, j = 0, 1, \dots, K-1$

and the corresponding parts of received samples are averaged over  $K$  parts. This

intra symbol time averaging reduce the variance of noise samples by  $K$  times. The

averaged received samples over  $K$  parts is given by

$$\mathbf{r}_{avg} = \frac{1}{K} \sum_{l=0}^{K-1} \mathbf{r}_l = \mathbf{p}_0' + \mathbf{w}_{avg} \quad (2.9)$$

where  $\mathbf{w}_{avg} = [w_{avg}[0], w_{avg}[1], \dots, w_{avg}[M-1]]$  with  $w_{avg}[i] = (1/K) \sum_{l=0}^{K-1} w[i + lM]$ .

$\{w_{avg}[i]\}$  are *iid* zero mean complex Gaussian random variables with variance  $\sigma_{t,avg}^2 = \sigma_t^2 / K$ . The FPTA [17] time domain channel estimation can be given by

$$\begin{aligned}\hat{h}_{FPTA}[n] &= (K/A)r_{avg}[n] \\ &= h[n] + (K/A)w_{avg}[n], \quad n = 0, 1, \dots, M-1\end{aligned}\quad (2.10)$$

The corresponding frequency response is

$$\hat{H}_{FPTA}[k] = FFT_N\{h_{FPTA}[n]\}, \quad k = 0, 1, \dots, N-1 \quad (2.11)$$

Pilot tones lie on several tones of an OFDM system. If we apply channel estimation method in Eq. (2.5), we can only obtain the frequency response of pilot tones. The rest of data tone must be obtained by interpolation. If we use FPTA channel estimation, the channel impulse response can be obtained first and the channel frequency response can be obtained by Fast Fourier transform of the estimated channel impulse response. We don't need interpolation in frequency domain.

## 2.2.2 Analysis of FPTA channel estimation error

We define channel estimation error in time domain as

$$e[n] = \hat{h}_{FPTA}[n] - h[n] = (K/A)w_{avg}[n]. \quad (2.12)$$

The variance of  $e[n]$  or Mean Square Error (MSE) of channel impulse response can be given as follows

$$\begin{aligned}\text{var}\{e[n]\} &= \text{mse}\{e[n]\} = E\{e[n]e^*[n]\} \\ &= \frac{K^2}{|A|^2} \sigma_{w,avg}^2 = \frac{K}{|A|^2} \sigma_w^2\end{aligned}\quad (2.13)$$

The corresponding channel estimation error in frequency domain can be obtained by Fast Fourier transform of  $e[n]$  and can be represented as follows

$$\begin{aligned}
e[k] &= FFT_N[e[n]] = \sum_{n=0}^{N-1} e[n]e^{-j2\pi kn/N} \\
&= \sum_{n=0}^{M-1} e[n]e^{-j2\pi kn/N}
\end{aligned} \tag{2.14}$$

The variance (MSE) of channel estimation in frequency domain can be written as

$$\begin{aligned}
\text{var}\{E[k]\} &= \text{mse}\{E[k]\} = E\{E[k]E^*[k]\} \\
&= \frac{N}{|A|^2} \sigma_w^2
\end{aligned} \tag{2.15}$$

In the next paragraph, the MST will be derived. The MSE of FPTA will compare with MSE of MST in next paragraph, and it will be shown that MST performs better than FPTA.

## 2.3 MST channel estimation

There may not be so many channel paths with significant strength in  $N$  samples interval of an OFDM symbol. Hence, among  $N$  samples (taps) of channel impulse response estimate, many samples (taps) will have little or no energy at all except noise perturbation. Neglecting those nonsignificant channel taps in channel estimation may introduce some performance degradation if some of the channel energy is missed, but at the same time it will eliminate the noise perturbation from those taps. Total noise perturbation from those neglected channel estimate taps are usually much higher than the multipath energy contained in them, especially for low SNR values. Hence, neglecting those nonsignificant channel estimate taps can improve the channel estimation performance significantly. There are two ways to select taps [17]. One is to select several significant taps, and the other is to select the taps which is above a threshold. If we select the channel taps, which are less than the real numbers of the

channel taps, we define this situation as missing tap or under-determined condition. In opposition to the missing taps, the selected channel taps, whose numbers are more than the real ones, are defined as over-determined condition. The error floor will occur in the under determined-condition. It is a serious problem in the performance of channel estimation. In this section, we want to derive the MSE performance of channel estimation under the condition of missing taps.

### 2.3.1 MST channel estimation algorithm

Training symbol of the MST approach is the same as the FPTA in Eq. (2.6) and Eq. (2.7). It contains  $K$  impulses and distributes uniformly in  $N$  samples of time domain. If the channel path gains remain essentially the same over an OFDM symbol interval, which is usually the case since OFDM symbol is often designed to satisfy this in order to maintain orthogonality among subcarriers, then the received samples corresponding to time-domain pilot samples contain  $K$  repeated version of scaled channel impulse response which are independently corrupted by AWGN. In order to choose most significant channel taps (MST), those  $K$  parts can be averaged so that the noise variance is reduced by  $K$  times and more reliable most significant channel taps can be obtained. In mathematical expression, the time-domain received samples corresponding to time-domain pilot samples can be given by

$$\begin{aligned}
 r[n] &= h[n] \otimes p[n] + w[n] \\
 &= \frac{A}{K} \sum_{m=0}^{K-1} h[n - mM] + w[n], \quad n = 0, 1, \dots, N-1
 \end{aligned} \tag{2.18}$$

Then averaging the received samples over  $K$  parts, we have the noise-corrupted scaled channel impulse response

$$r_{avg}[n] = \frac{A}{K}h[n] + w_{avg}[n], \quad n = 0, 1, \dots, M-1$$

The FPTA channel impulse response estimation is given by

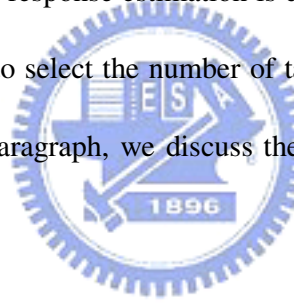
$$\hat{h}_{FPTA}[n] = \frac{K}{A}r_{avg}[n] = h[n] + \frac{K}{A}w_{avg}[n], \quad n = 0, 1, \dots, M-1 \quad (2.19)$$

After channel impulse response is estimated by the FPTA algorithm, the most significant  $J$  channel delay taps are chosen for the MST channel estimation.

Suppose the time indices of the most significant  $J$  taps are  $n_0, n_1, \dots, n_{J-1}$ . The MST method is obtained by setting the other channel taps gains to zero as shown below

$$\hat{h}_{MST}[n] = \sum_{i=0}^{J-1} \hat{h}_{FPTA}[n_i] \delta[n - n_i], \quad n = 0, 1, \dots, N-1 \quad (2.20)$$

The corresponding frequency response estimation is directly obtained by Fast Fourier transform of  $\hat{h}_{MST}[n]$ . How to select the number of taps  $J$  is an important problem in MST algorithm. In next paragraph, we discuss the selection of  $J$  by analysis of MSE for channel estimation.



### 2.3.2 Analysis of MST channel estimation error

In the mean square error analysis, we consider the over determined condition in which  $J$  is larger than total number of delay taps  $L$ . Recall Eq. (2.20), the estimated channel impulse response by the MST can be written as

$$\begin{aligned} \hat{h}_{MST}[n] &= \sum_{i=0}^{J-1} \hat{h}_{FPTA}[n_i] \delta[n - n_i] \\ &= h[n] + \frac{K}{A} \sum_{i=0}^{J-1} w_{avg}[n_i] \delta[n - n_i] \end{aligned} \quad (2.21)$$

The estimated frequency response can be obtained as follows



$$\hat{H}_{MST}[k] = H[k] + \frac{K}{A} \sum_{n=0}^{N-1} \sum_{i=0}^{J-1} w_{avg}[n_i] \delta[n - n_i] e^{-j2\pi kn/N} \quad (2.22)$$

The MSE in frequency response is

$$\begin{aligned} mse\{H[k]\} &= E\{|H[k] - \hat{H}_{MST}[k]|^2\} \\ &= \frac{K^2}{A^2} J \sigma_{i,avg}^2 = \frac{KJ}{N} mse\{H_{FPTA}\} \end{aligned} \quad (2.23)$$

The MSE performance gain of the MST method over FPTA method is ideally  $KJ/N$ .

The smaller  $J$  gets the better performance of MSE, but  $J$  must be larger or equal to  $L$ . The best choice of  $J$  is set to  $L$ .

Now, we extend the analysis of MSE to under determined condition ( $J < L$ ). The estimated channel impulse response by the MST can be written as

$$\begin{aligned} \hat{h}_{MST}[n] &= \sum_{i=0}^{J-1} \hat{h}_{LS}[n_i] \delta[n - n_i] \\ &= h[n] - \sum_{m=J}^{L-1} h[n] \delta[n - n_m] + \frac{K}{A} \sum_{i=0}^{J-1} w_{avg}[n_i] \delta[n - n_i] \end{aligned} \quad (2.24)$$

The estimated frequency response can be obtained as follow

$$\begin{aligned} \hat{H}_{MST}[k] &= H[k] - \sum_{n=0}^{N-1} \sum_{m=J}^{L-1} h[n] \delta[n - n_m] e^{-j2\pi kn/N} \\ &\quad + \frac{K}{A} \sum_{n=0}^{N-1} \sum_{i=0}^{J-1} w_{avg}[n_i] \delta[n - n_i] e^{-j2\pi kn/N} \end{aligned} \quad (2.25)$$

The MSE in frequency response is

$$\begin{aligned} mse\{\hat{H}_{MST}[k]\} &= E\{|H[k] - \hat{H}_{MST}[k]|^2\} \\ &= \sum_{m=J}^{L-1} \sigma_{h[n_m]}^2 + \frac{KJ}{N} mse\{H_{FPTA}\} \end{aligned} \quad (2.26)$$

where  $\sigma_{h[n_m]}^2$  is the power delay profile for the  $n_m$ th propagation delay path. The error floor occurs in this case because of missing tap. The channel estimation error caused by the noise from an additional tap in channel estimation is much less than that caused by missing one tap of the multipaths. The choice of the number of most

significant taps  $J$  must be larger than the number of multipaths to prevent channel estimation error caused by missing taps. A suitable choice [17] for  $J$  may be two times or more of the number of multipaths. Another MST tap selection can be implemented by selecting the channel taps whose energy is above a threshold [17]. The threshold may be set as  $\eta$  times the maximum channel tap's energy. In the simulation results, we can find the suitable choice of  $\eta$  depend on the operating SNR. A suitable choice of  $\eta$  is 20dB below  $1/\text{SNR}$ . MST improves performance of FPTA by noise suppression. If the channel taps is small. MST algorithm gains more noise suppression by selecting fewer taps. Comparing the outdoor mobile channel with the indoor wireless channel, there are fewer channel taps in the outdoor mobile channel than in the indoor mobile channel. Therefore, the MST algorithm is suitable for the outdoor mobile channel better than the indoor wireless channel.



## 2.4 FPTA with LMMSE channel estimation

In Section 2.3, we use MST algorithm to improve FPTA channel estimation. In this section we will introduce another channel estimation method, based on correlation of channel, to improve FPTA channel estimation. This channel estimation method is called LMMSE [18]. The performance of MST with matched selection of taps, selected numbers of taps is equal to the real number of taps, is the same as the performance of LMMSE.

### 2.4.1 LMMSE channel estimation algorithm

FPTA channel estimation method can also be improved by using linear minimum mean square error (LMMSE) [18]. In LMMSE channel estimation, we need to know the autocorrelation matrix of  $\hat{\mathbf{h}}_{FPTA}$  and the cross correlation matrix between  $\hat{\mathbf{h}}_{FPTA}$  and  $\mathbf{h}$ .  $\hat{\mathbf{h}}_{FPTA} = [\hat{h}_{FPTA}[0], \hat{h}_{FPTA}[1], \dots, \hat{h}_{FPTA}[M-1]]^T$  is the estimated impulse response with FPTA.  $\mathbf{h} = [h[0], h[1], \dots, h[M-1]]^T$  is the true channel impulse response. If we define the autocorrelation matrix  $\mathbf{R}_{\hat{h}\hat{h}}$  and cross correlation  $\mathbf{R}_{hh}$  as

$$\mathbf{R}_{\hat{h}\hat{h}} = E\{\hat{\mathbf{h}}_{FPTA}\hat{\mathbf{h}}_{FPTA}^H\} \quad (2.28)$$

$$\mathbf{R}_{hh} = E\{\mathbf{h}\mathbf{h}^H\} \quad (2.29)$$

We can write LMMSE channel estimation [18] as

$$\hat{\mathbf{h}}_{mmse} = \mathbf{R}_{hh}\mathbf{R}_{\hat{h}\hat{h}}^{-1}\hat{\mathbf{h}}_{FPTA} \quad (2.30)$$

Lets us consider a wide-sense stationary uncorrelated scattering (WSSUS) multipath channel with power delay profile given by  $\sigma_{h_i}^2$  at delays of  $i$  OFDM sample intervals. Due to the uncorrelated multipaths, the correlation matrix of channel impulse response  $\mathbf{R}_{hh}$  becomes a diagonal matrix with the diagonal elements given by the power delay profile. The Eq. (2.28) can be rewritten as

$$\hat{\mathbf{h}}_{mmse} = \text{diag}\left\{\frac{\sigma_{h_0}^2}{\sigma_{h_0}^2 + \beta / SNR}, \frac{\sigma_{h_1}^2}{\sigma_{h_1}^2 + \beta / SNR}, \dots, \frac{\sigma_{h_{N-1}}^2}{\sigma_{h_{N-1}}^2 + \beta / SNR}\right\}\hat{\mathbf{h}}_{FPTA} \quad (2.31)$$

where  $SNR/\beta$  in Eq. (2.31) is replaced by  $\sigma_w^2(|A|K)^{-2}$ ,  $\sigma_w^2$  denotes the noise variance in time domain and  $K$  is the number of impulses in a training symbol. Compared to MST with LMMSE, LMMSE needs more computation on estimation of

channel correlation and noise power. We can find the performance of MST with matched selection of taps in simulation results is similar to the performance of LMMSE in simulation results. MST has lower complexity than LMMSE, MST seems to be a better choice than LMMSE. But in general, we don't know how many taps in the channel. In next Chapter, we consider the time varying channel. The decision directed algorithm [19], linear interpolation [13], and polynomial interpolation [14] will be implemented by FPTA and MST. Furthermore, in fast fading assumption, sub-symbol polynomial interpolation is proposed. The sub-symbol polynomial interpolation apply MST algorithm to reduce complexity and do noise suppression.



# Chapter 3

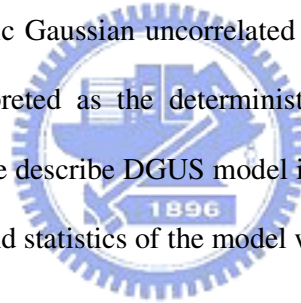
## Time Varying Channel Tracking

In Chapter 2, we introduced the FPTA method and MST method for channel estimation. They work fine in time invariant channel. In this Chapter, The serious problem, mobile fading channel, in channel estimation will be discussed. The channel impulse responses change in different time slot (One OFDM symbol is divided into several time slots) of one OFDM symbol. The estimated channel impulse response of the training symbol is an improper channel estimation for data symbols in time varying channel assumption. In order to solve this problem, the sub-symbol polynomial interpolation algorithm will be proposed. We suppose every delay tap of impulse response change in every time slot and is close to a polynomial function. The polynomial interpolation utilizes LS channel estimation in training symbol to get the coefficients of polynomial function. Then it interpolates the channel impulse response in data symbol. The estimation error is divided into two parts. One is noise error, caused from the noise of the system. The other is model error, which is generated by the difference between real channel impulse and polynomial model. Because the model error is relative to the statistics of channel, we use a time varying channel model in Section 3.1. The statistics of channel will be derived and utilized to check performance of model error. Furthermore, we can mitigate noise effect of the LS

channel estimation in training symbol by Wiener filter. It makes some improvements for higher-order polynomials. We also compare other existing time varying channel estimation methods in this Chapter including decision directed algorithm, linear interpolation, and time-frequency domain polynomial interpolation. The performance of these channel estimation method will be shown in Chapter 4.

## 3.1 Time varying channel model

The concept of deterministic channel modeling [20] has recently been extended [21] to frequency-selective mobile radio channels, resulting in a new class of model processes, called deterministic Gaussian uncorrelated scattering (DGUS) model. The DGUS model can be interpreted as the deterministic counterpart of Bello's [22] stochastic WSSUS model. We describe DGUS model in equivalent complex baseband. The function of the system and statistics of the model will be introduced latter.



### 3.1.1 DGUS channel model

The time variant impulse response of the DGUS model is given by a sum of  $L$  discrete delay paths, according to

$$h(\tau, t) = \sum_{l=0}^{L-1} a_l \mu_l(t) \delta(\tau - \tau_l) \quad (3.1)$$

where the real-valued  $a_l$  are called delay coefficients,  $\mu_l(t)$  are complex deterministic Gaussian process, and  $\tau_l$  are discrete propagation delays. Both the delay coefficients  $a_l$  and the discrete propagation delays  $\mu_l(t)$  determine the delay

power spectral density of frequency–selective deterministic channel models. Strictly speaking, the delay coefficient is a measure of the square root of the average delay power, which is assigned to the  $l$ th path discrete propagation path. The channel disturbance of the Doppler effect, caused by the relative motion between the receiver and the transmitter, are modeled in Eq. (3.2) by complex deterministic Gaussian processes.

$$\mu_l(t) = \sum_{n=1}^{N_l} c_{n,l} e^{j(2\pi f_{n,l}t + \theta_{n,l})} \quad (3.2)$$

where  $l = 0, 1, \dots, L-1$ .  $N_l$  denotes the number of harmonic functions, assigned to the  $l$ th path,  $c_{n,l}$  is the Doppler coefficient of the  $n$ th component of the  $l$ th propagation path, and  $f_{n,l}$  and  $\theta_{n,l}$  are the corresponding discrete Doppler frequency and Phase. The time-varying channel impulse response  $h(t, \tau)$  is completely deterministic. Therefore, the correlation properties of  $h(t, \tau)$  are derived from time average, instead of statistical averages. Figure 3.1 shows the structure of the complex Gaussian random process  $\mu_l(t)$  in the continuous-time representation.

To ensure that the simulation model which is derived below has the same striking properties as a uncorrelated scattering (US) model, the complex deterministic Gaussian processes must be uncorrelated for different propagation delays, i.e., the deterministic process  $\mu_l(t)$  and  $\mu_\lambda(t)$  have to be designed in such a way that they are uncorrelated for  $l \neq \lambda$ , where  $l, \lambda = 0, 1, \dots, L-1$ . This demand can be fulfilled easily if the discrete Doppler frequencies  $f_{n,l}$  are chosen in such a way that the sets  $\{\pm f_{n,l}\}$  and  $\{\pm f_{m,\lambda}\}$  are mutually disjoint for different propagation delays. Thus, the US condition can be expressed by

$$US \Leftrightarrow f_{n,l} \neq \pm f_{m,\lambda} \text{ for } l \neq \lambda \quad (3.3)$$

where  $n = 1, 2, \dots, N_l$ ,  $m = 1, 2, \dots, N_\lambda$ , and  $l, \lambda = 0, 1, \dots, L - 1$ .

### 3.1.1 Statistic properties of DGUS channel

In the following paragraph, we derive the correlation properties of the deterministic Gaussian process Eq. (3.2)

$$r_{\mu_l \mu_\lambda}(\tau') := \lim_{T \rightarrow \infty} \frac{1}{2T} \int_{-T}^T \mu_l^*(t) \mu_\lambda(t + \tau') dt \quad (3.4)$$

can be expressed in closed form by

$$r_{\mu_l \mu_l}(\tau') = \sum_{n=1}^{N_l} c_{n,l}^2 e^{j2\pi f_{n,l} \tau'}, \quad \text{if } l = \lambda \quad (3.5a)$$

$$r_{\mu_l \mu_\lambda}(\tau') = 0, \quad \text{if } l \neq \lambda \quad (3.5b)$$

where  $l, \lambda = 0, 1, \dots, L - 1$ .  $r_{\mu_l \mu_\lambda}(\tau')$  is the autocorrelation function of the deterministic Gaussian process  $\mu_l(t)$  defined by Eq.(3.2). Next, we define the Fourier transform of autocorrelation function of deterministic Gaussian process  $r_{\mu_l \mu_l}(\tau')$

$$\begin{aligned} S_{\mu_l \mu_l}(f) &= \int_{-\infty}^{\infty} r_{\mu_l \mu_l}(\tau') e^{j2\pi f \tau'} d\tau' \\ &= \sum_{n=1}^{N_l} c_{n,l}^2 \delta(f - f_{n,l}) \end{aligned} \quad (3.6)$$

The  $S_{\mu_l \mu_l}(f)$  is called the Doppler power spectral density of the  $l$ th propagation path. Without the loss of generality, the area of  $S_{\mu_l \mu_l}(f)$  over all frequency is equal to one. The Doppler coefficients  $c_{n,l}$  must satisfy the following condition

$$\sum_{n=1}^{N_l} c_{n,l}^2 = 1 \quad (3.7)$$

for  $l = 0, 1, \dots, L - 1$ . In a typical mobile system, the Doppler power spectral density



can be expressed as

$$S_{\mu_i\mu_i}(f) = \begin{cases} \frac{k}{\sqrt{f_{D,l}^2 - f^2}} & |f| \leq f_{D,l} \\ 0 & |f| > f_{D,l} \end{cases} \quad (3.8)$$

where  $k$  is a constant which depends on the average power of the deterministic Gaussian process  $\mu_i(t)$ , and  $f_{D,l}$  is the maximum Doppler frequency. Then combining Eq. (3.6) and Eq. (3.8), we can get the following equation

$$\tilde{c}_{n,l}^2 = \frac{k}{\sqrt{f_{D,l}^2 - f_{n,l}^2}} \quad (3.9)$$

We also have to satisfy the Eq. (3.7) condition. Finally, the Doppler coefficients  $c_{n,l}$  can be obtained from the discrete Doppler frequencies  $f_{n,l}$ .

$$\tilde{c}_{n,l}^2 = \frac{1}{\sqrt{f_{D,l}^2 - f_{n,l}^2}} \frac{1}{\sum_{n=1}^{N_l} \frac{1}{\sqrt{f_{D,l}^2 - f_{n,l}^2}}} \quad (3.10)$$


where  $n = 1, 2, \dots, N_l$ ,  $l = 0, 1, \dots, L-1$ . The Doppler power spectral density  $S_{\mu\mu}(f)$  of DGUS channel can be determined from the Doppler power spectral density for  $l$  th propagation path.

$$S_{\mu\mu}(f) = \sum_{l=0}^{L-1} a_l^2 S_{\mu_i\mu_i}(f) \quad (3.11)$$

The average Doppler shift of the DGUS model  $D_{\mu\mu}^{(1)}$  is defined by the first moment of  $S_{\mu\mu}(f)$ , i.e.,

$$\begin{aligned}
D_{\mu\mu}^{(1)} &:= \frac{\int_{-\infty}^{\infty} f S_{\mu\mu}(f) df}{\int_{-\infty}^{\infty} S_{\mu\mu}(f) df} \\
&= \frac{\sum_{l=0}^{L-1} a_l^2 [\sum_{n=1}^{N_l} f_{n,l} c_{n,l}^2]}{\sum_{l=0}^{L-1} a_l^2 [\sum_{n=1}^{N_l} c_{n,l}^2]}
\end{aligned} \tag{3.12}$$

The Doppler spread  $D_{\mu\mu}^{(2)}$  of DGUS model is defined by the square root of the second central moment of  $S_{\mu\mu}(f)$ , i.e.,

$$\begin{aligned}
D_{\mu\mu}^{(2)} &:= \sqrt{\frac{\int_{-\infty}^{\infty} (f - D_{\mu\mu}^{(1)})^2 S_{\mu\mu}(f) df}{\int_{-\infty}^{\infty} S_{\mu\mu}(f) df}} \\
&= \sqrt{\frac{\sum_{l=0}^{L-1} a_l^2 [\sum_{n=1}^{N_l} (f_{n,l} c_{n,l})^2]}{\sum_{l=0}^{L-1} a_l^2 [\sum_{n=1}^{N_l} c_{n,l}^2]} - (D_{\mu\mu}^{(1)})^2}
\end{aligned} \tag{3.13}$$



## 3.2 The FPTA and the MST method in time varying channel

In this section, we introduce two channel estimation methods whose don't need statistic of channel in the time varying channel. One is decision direct algorithm, the other is linear interpolation. In the decision direct algorithm, the initial channel estimation in training symbol is obtained by FPTA or MST. Then decision direct algorithm [19] is used to track the channel in the data position. In the linear interpolation, channel in training symbol is also estimated by FPTA or MST. Then we do linear interpolation by two neighbor training channel which is estimated with

FPTA or MST.

### 3.2.1 FPTA and MST with decision direct algorithm

The corresponding channel frequency response estimation of the FPTA method or the MST method is N-points Fast Fourier transform of  $\hat{\mathbf{h}}_{FPTA}$  or  $\hat{\mathbf{h}}_{MST}$ . A simple decision directed method will be introduced. It is called one-tap Recursive Least Squares filter [19]. The algorithm is

$$\begin{aligned}\hat{H}(m,k) &= \alpha \frac{R(m,k)}{\hat{X}(m,k)} + (1-\alpha)\hat{H}(m-1,k) \\ Z(m,k) &= \frac{R(m,k)}{\hat{H}(m-1,k)}\end{aligned}\quad (3.14)$$

where  $R(m,k)$  is the received symbol at  $k$ th subcarrier and  $m$ th data symbol;  $\hat{X}(m,k)$  is the estimation of the constellation at  $k$ th subcarrier and  $m$ th data symbol;  $\hat{H}(m,k)$  is the estimation of the demodulated channel;  $Z(m,k)$  is the decision variable (a noisy estimate of the constellation value  $X(m,k)$ ) and  $\alpha$  is the update factor in the estimation of the channel. The algorithm is also shown in Figure 3.1.

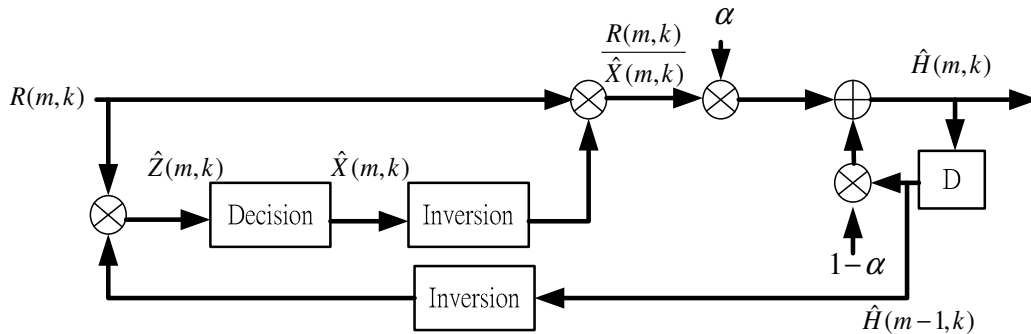


Fig. 3.1 Block of One-tap Recursive Least Square filter

The initial channel estimation can be completed by training symbol (FPTA or MST), then update the channel by the one-tap Recursive Least Squares filter. Periodic resending of the training symbol will reorient the estimation of the channel to the correct position. The errors will typically occur when the signal is in a deep fade.

### 3.2.2 FPTA and MST with linear interpolation algorithm

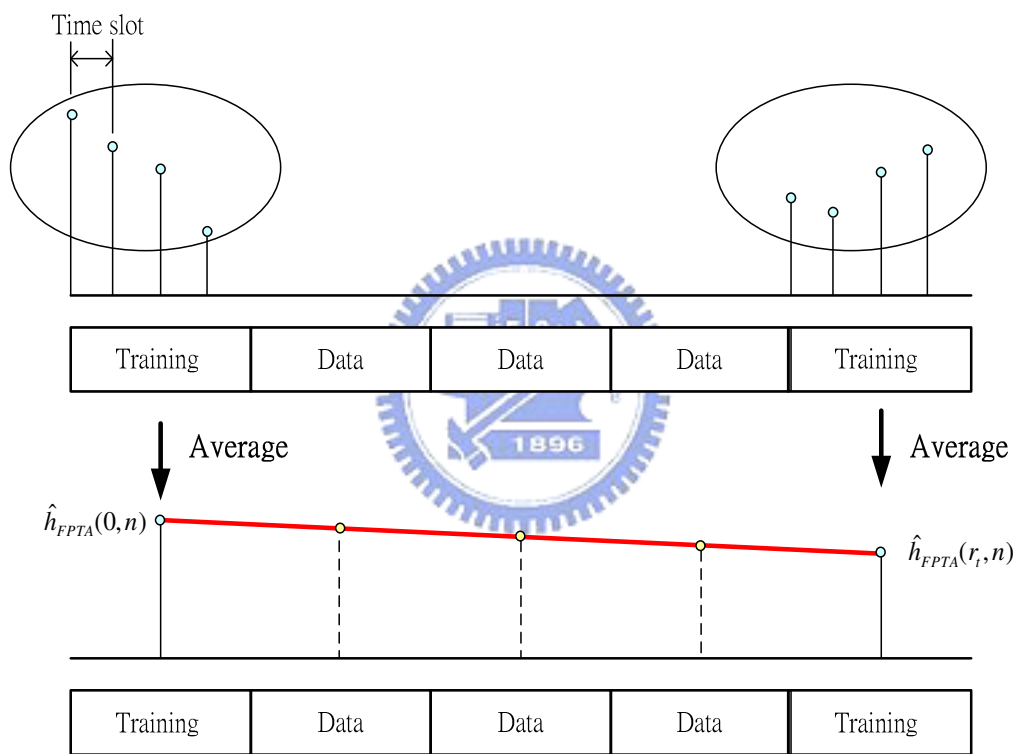


Fig. 3.2 Illustration of linear interpolation

In FPTA or MST methods, we use the channel that is estimated by training symbol to recover data. The mobile fading channel changes with time. The channel of training symbol is different from the channel of data symbol. Even the channel of training symbol can be estimated very accurately, it still can't be used to recover data. Fortunately, because the channel doesn't change rapidly in short-time intervals or in low Doppler frequency mobile environment, then we can suppose that the channel

presents the linear change between two training signals both in the time domain and in the frequency domain. Figure 3.2 shows the illustration of linear interpolation. First, we estimate channel of training symbol by FPTA or MST. The estimated channels of two adjacent training symbols can be used to make a straight line, then we can interpolate channel of data symbols by this straight line. The linear interpolation [13] can be carried out in two domains. One is the interpolation in the time domain, which is achieved by the linear interpolation in delay propagation path. The other is interpolation in the frequency domain, which is achieved by linear interpolation in subcarriers. If We insert training symbol in every  $r_t$  OFDM symbols, in the time domain, the linear interpolation for  $n$  th propagation path in  $m$  th OFDM symbol can be shown as

$$\hat{h}_{Linear}(m, n) = \frac{r_t - m}{r_t} \hat{h}_{FPTA}(0, n) + \frac{m}{r_t} \hat{h}_{FPTA}(r_t, n) \quad (3.15)$$

where  $n = 0, 1, \dots, M - 1$ ;  $m = 1, 2, \dots, r_t - 1$ , and  $\hat{h}_{FPTA}(m, n)$  is FPTA channel estimation for  $n$  th propagation path in  $m$  th training symbol. In the frequency domain, the linear interpolation for  $m$  th OFDM symbol can be shown as

$$\hat{H}_{Linear}(m, k) = \frac{r_t - m}{r_t} \hat{H}_{FPTA}(0, k) + \frac{m}{r_t} \hat{H}_{FPTA}(r_t, k), \quad (3.16)$$

where  $k = 0, 1, \dots, N - 1$ , and  $\hat{H}_{FPTA}(m, k)$  is  $k$  th tone of Fast Fourier transform of FPTA channel estimation in  $m$  th OFDM symbol. The performance of the time domain interpolation and the one of the frequency domain interpolation are the same because frequency domain interpolation can be obtained by Fast Fourier transform of the time domain interpolation. The difference between these two domain interpolations is that the time domain interpolation is less complex, due to the numbers of multipaths are much less than the tones of an OFDM symbol. There is a

less complex way. Using MST algorithm is much more convenient than using FPTA.

The linear interpolation based on MST channel estimation can be obtained by

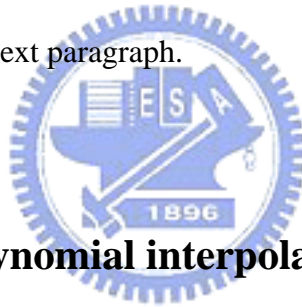
$$\begin{aligned}\hat{h}_{Linear}(m, n_l) &= \frac{r_t - m}{r_t} \hat{h}_{MST}(0, n_l) + \frac{m}{r_t} \hat{h}_{MST}(r_t, n_l), \quad l = 0, 1, \dots, J-1 \\ \hat{h}_{Linear}(m, n_l) &= 0, \quad l \geq J\end{aligned}\quad (3.17)$$

where  $\hat{h}_{MST}(m, n_l)$  is MST channel estimation for  $n_l$ th propagation path in  $m$ th training symbol. And  $n_l$  is delay length, corresponding to  $l$ th significant delay path of MST algorithm;  $m$  represents time index of OFDM symbols. Besides, the noise suppression is the advantage of the linear interpolation based on MST algorithm. Comparing to the decision directed algorithm with the linear interpolation, the decision directed algorithm must demodulate the decision variable to obtain the estimation of the constellation point. In our simulation, 64 QAM modulation is used. The estimation of the constellation will fail easily. The demodulation of 64-QAM also cost a lot of computation. The linear interpolation is a more suitable choice than decision directed algorithm. The linear interpolation models variation of channel as linear change. A more general variation of channel is a polynomial model. We propose a sub-symbol polynomial interpolation in next paragraph.

### 3.3 Sub-symbol polynomial interpolation

The channel variation in physical world is smooth in both the time domain and the frequency domain. Such a smooth varying function can be approximated by projecting to a finite set of basis functions. Moreover, since the OFDM channel parameters are located in a time-frequency plane, it is natural to approach the channel frequency response over a time-frequency window to a small set of polynomial basis

functions [14]. The numbers of subcarriers are usually greater than the number of channel delay taps. We may only approach the delay tap over a time window to a small set of polynomial basis function in order to save computation. The number and positions of delay taps can be selected by choosing the most significant taps selection which is introduced in Chapter 2. Further more, in the fast fading channel, we can obtain channel time varying information by using training symbol of FPTA. Compared to FPTA, we don't average the received training symbol. The channel can be estimated in different time slot. Then we use these channel impulse responses to make a polynomial function which is closest to channel impulse response, which estimated by training symbol. We defined this channel estimation method as sub-symbol polynomial interpolation. The algorithm of sub-symbol polynomial interpolation is performed in next paragraph.



### **3.3.1 Sub-symbol polynomial interpolation algorithm**

The form of the training symbol of the sub-symbol polynomial interpolation is similar with that of FPTA. In the FPTA method, we assume that the channel impulse response is unchanged in an OFDM symbol, and it can be estimated by averaging  $K$  identical parts (time slot) of received training symbol. In the sub-symbol polynomial interpolation, we assume that the channel impulse response change  $K$  times (time slots) in an OFDM symbol. Averaging of training symbol is not necessary. Because the time slot of the received training symbol preserves time varying information. Then we can do a curve fitting to approach the channel on data location (seen in Figure 3.3).

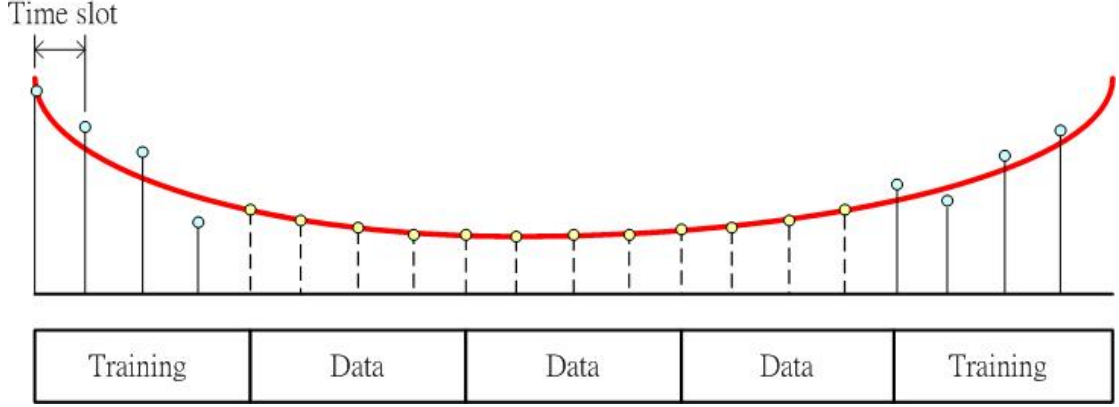


Fig. 3.3 Channel tracking by sub-symbol polynomial interpolation

In the following we will derive sub-symbol polynomial interpolation algorithm.

Now, we model  $l$  th propagation path change with time as a polynomial function.

$$h_{poly}(t, l) = \mathbf{a}_q(t) \mathbf{b}_q(l) \quad (3.18)$$

where  $\mathbf{a}_q(t)$  is time vector,  $\mathbf{a}_q(t) = [1, t, t^2, \dots, t^q]$ ,  $q$  is the order of polynomial function;  $\mathbf{b}_q(l) = [b_0(l), b_1(l), \dots, b_q(l)]^T$  is the coefficient vector for  $l$  th propagation path. Afterwards, we recall Eq. (2.8) and find the LS channel estimation for every time slot of training symbol as follows

$$\begin{aligned} \hat{\mathbf{h}}_{LS} &= \mathbf{r} / A = [\hat{\mathbf{h}}_{LS}(1), \hat{\mathbf{h}}_{LS}(2), \dots, \hat{\mathbf{h}}_{LS}(K)] \\ &= [\mathbf{h}(1), \mathbf{h}(2), \dots, \mathbf{h}(K)] + \mathbf{w} / A \end{aligned} \quad (3.19)$$

where  $A$  is the pilot amplitude and  $\hat{\mathbf{h}}_{LS}(t) = [\hat{h}_{LS}(t, 0), \hat{h}_{LS}(t, 1), \dots, \hat{h}_{LS}(t, M-1)]$ . The coefficients of the polynomial function can be estimated by two neighbor training symbols, according to the following criterion

$$\text{Min}_{\mathbf{b}_q(l)} \sum_{t_p \in P} [\hat{h}_{LS}(t_p, l) - \mathbf{a}_q(t_p) \mathbf{b}_q(l)]^2 \quad (3.20)$$

where the set  $P$  contains the time slot index of training symbol in the time window, and  $\hat{h}_{LS}(t_p, l)$  is LS channel estimation of  $l$  th delay path in  $t_p$  th time slot.



window, and  $\hat{h}_{LS}(t_p, l)$  is LS channel estimation of  $l$  th delay path in  $t_p$  th time slot.

The polynomial coefficients vector can be estimated as

$$\hat{\mathbf{b}}_q(l) = \mathbf{A}_{T,q}^\perp \tilde{\mathbf{h}}_{LS}(l) \quad (3.21)$$

where  $\mathbf{A}_{T,q}$  is called training time matrix, every row of  $\mathbf{A}_{T,q}$  is the time vector, corresponding to time slot index of training symbols in the time window.  $\mathbf{A}_{T,q}^\perp$  is the pseudo inverse of  $\mathbf{A}_{T,q}$ , and

$$\begin{aligned} \tilde{\mathbf{h}}_{LS}(l) &= [\hat{h}_{LS}(0, l), \hat{h}_{LS}(1, l), \dots, \hat{h}_{LS}(K-1, l), \\ &\quad \hat{h}_{LS}(Kr_t, l), \hat{h}_{LS}^{(n+1)}(Kr_t+1, l), \dots, \hat{h}_{LS}^{(n+1)}(Kr_t+K-1, l)]^T \\ &= [\tilde{\mathbf{h}}_{LS}^{(1)}(l)^T, \tilde{\mathbf{h}}_{LS}^{(2)}(l)^T]^T \end{aligned} \quad (3.22)$$

where

$$\begin{aligned} \tilde{\mathbf{h}}_{LS}^{(1)}(l) &= [\hat{h}_{LS}(0, l), \hat{h}_{LS}(1, l), \dots, \hat{h}_{LS}(K-1, l)]^T \\ \tilde{\mathbf{h}}_{LS}^{(2)}(l) &= [\hat{h}_{LS}(Kr_t, l), \hat{h}_{LS}^{(n+1)}(Kr_t+1, l), \dots, \hat{h}_{LS}^{(n+1)}(Kr_t+K-1, l)]^T \end{aligned}$$

$r_t$  is the inverse of training rate. We can achieve channel interpolation of data time slot of  $l$  th delay path using by

$$\hat{h}_{poly}(t_D, l) = \mathbf{a}_q(t_D) \hat{\mathbf{b}}_q(l), \quad t_D \in D \quad (3.23)$$

where the set  $D$  contains the time slot index of data symbol in the time window. The impulse response of  $t_D$  th time slot can be constructed by

$$\hat{\mathbf{h}}_{poly}(t_D) = [\hat{h}_{poly}(t_D, 1), \hat{h}_{poly}(t_D, 2), \dots, \hat{h}_{poly}(t_D, M-1)]^T \quad (3.24)$$

Besides, we can obtain the estimated  $l$  th path impulse response at all data position by

$$\hat{\mathbf{h}}_{poly}(l) = \mathbf{A}_{D,q} \hat{\mathbf{b}}_q(l) \quad (3.25)$$

where  $\mathbf{A}_{D,q}$  is called data time matrix; every row of  $\mathbf{A}_{D,q}$  is the time vector, which corresponds to time slot of data symbol. There are  $K$  channel impulse responses,

interpolated by polynomial interpolation. By averaging  $K$  interpolated channel impulse responses [13], it is simple to present the channel impulse response of an OFDM symbol. In the low SNR environment, the polynomial function makes a huge error by tracking the noise perturbation. We can mitigate the noise perturbation by using Wiener filter. The LS estimation can be improved by the Wiener filter and more accurate coefficients of polynomial function can be found. The smoothed channel of  $m$  th training symbol  $\hat{\mathbf{h}}_{mmse}^{(m)}(l)$  can be shown as follows

$$\begin{aligned} \tilde{\mathbf{h}}_{mmse}^{(m)}(l) &= \mathbf{R}_{ll} \left( \mathbf{R}_{ll} + \frac{\sigma_t^2}{|A|^2} \mathbf{I} \right)^{-1} \tilde{\mathbf{h}}_{LS}^{(m)}(l) \\ &= \mathbf{D} \begin{bmatrix} \frac{\lambda_1}{\lambda_1 + \sigma_t^2 / |A|^2} & 0 & 0 \\ 0 & \ddots & 0 \\ 0 & 0 & \frac{\lambda_K}{\lambda_K + \sigma_t^2 / |A|^2} \end{bmatrix} \mathbf{D}^H \tilde{\mathbf{h}}_{LS} \end{aligned} \quad (3.26)$$

where  $\mathbf{R}$  is the autocorrelation matrix of channel impulse response of  $l$  th propagation path.  $\lambda_i$  and  $\mathbf{D}$  are the eigenvalue and eigenmatrix of  $\mathbf{R}_{ll}$ . In the low SNR environment, the channel is smoothed by Wiener filter about 10dB, better than the LS estimation in MSE performance. After smoothing,  $\tilde{\mathbf{h}}_{LS}(l)$  is replaced by  $\tilde{\mathbf{h}}_{mmse}(l)$  in Eq. (3.21) to estimate polynomial coefficients. Where  $\tilde{\mathbf{h}}_{mmse}(l) = [\tilde{\mathbf{h}}_{mmse}^{(1)}(l)^T, \tilde{\mathbf{h}}_{mmse}^{(2)}(l)^T]^T$ . After that, the channel interpolation is smoothed by Wiener filter, and polynomial interpolation are obtained by

$$\hat{\mathbf{h}}_{mmse}(k_D, l) = \mathbf{a}_q(k_D, l) \hat{\mathbf{b}}_{mmse}(l) \quad (3.27)$$

$$\hat{\mathbf{h}}_{mmse}(k_D, l) = [\hat{h}_{mmse}(k_D, l), \hat{h}_{mmse}(k_D, l), \dots, \hat{h}_{mmse}(k_D, l)] \quad (3.28)$$

### 3.3.2 The MST algorithm for polynomial interpolation

The MST algorithm can also be employed to reduce computation complexity and noise perturbation in the time domain interpolation. The most significant paths can be chosen by the FPTA channel estimation in  $n$ th training symbol. The most significant  $J$  taps are chosen as the  $J$  largest amplitude channel taps. Let the channel tap indexes for those most significant  $J$  propagation path be denoted by  $\tau_0, \tau_1, \dots, \tau_{J-1}$ . The selected tap indexes are utilized to  $n$ th and  $n+1$ th training symbol. The rest of the channel taps are setting to zero. The number of multipath reduces from  $M$  to  $J$ . The reconstructed LS estimation can be shown as

$$\hat{\mathbf{h}}_{MST} = [\hat{\mathbf{h}}_{MST}(1), \hat{\mathbf{h}}_{MST}(2), \dots, \hat{\mathbf{h}}_{MST}(K-1)] \quad (3.29)$$

where

$$\hat{\mathbf{h}}_{MST}(t) = [h_{MST}(t,0), h_{MST,1}(t,1), \dots, h_{MST,M-1}(t, M-1)] \quad (3.30)$$

and  $\hat{h}_{MST}(t, n) = h_{LS}(t, n)\delta[n - \tau_i]$ . The polynomial coefficients vector of  $l$ th path can be estimated as

$$\hat{\mathbf{b}}_q(l) = \mathbf{A}_{T,q}^\perp \tilde{\mathbf{h}}_{MST}(l) \quad (3.31)$$

where  $\mathbf{A}_{T,q}$  is called training time matrix; every row of  $\mathbf{A}_{T,q}$  is the time vector, corresponding to time slot index of training symbols in the time window.  $\mathbf{A}_{T,q}^\perp$  is the pseudo inverse of  $\mathbf{A}_{T,q}$ , and

$$\tilde{\mathbf{h}}_{MST}(l) = [\hat{h}_{MST}(0, l), \hat{h}_{MST}(1, l), \dots, \hat{h}_{MST}(K-1, l), \hat{h}_{MST}(Kr_t, l), \hat{h}_{MST}(Kr_t+1, l), \dots, \hat{h}_{MST}(Kr_t+K-1, l)]^T \quad (3.32)$$

is the most significant selected taps of LS channel estimation vector for  $l$ th propagation delay path. The channel interpolation of data time slot of  $l$ th propagation path can be achieved by

$$\hat{h}_{poly}(t_D, l) = \mathbf{a}_q(t_D) \hat{\mathbf{b}}_q(l), \quad k_D \in D \quad (3.33)$$

where the set  $D$  contains the time slot index of data symbol in the time window. The impulse response of  $t_D$  th time slot in the time window can be constructed by

$$\hat{\mathbf{h}}_{poly}(t_D) = [\hat{h}_{poly}(t_D, 0), \hat{h}_{poly}(t_D, 1), \dots, \hat{h}_{poly}(t_D, M-1)]^T \quad (3.34)$$

We can obtain the estimated  $l$  th path impulse response at all data position by

$$\hat{\mathbf{h}}_{poly}(l) = \mathbf{A}_{D,q} \hat{\mathbf{b}}(l) \quad (3.35)$$

where  $\mathbf{A}_{D,q}$  is called data time matrix; every row of  $\mathbf{A}_{D,q}$  is the time vector, corresponding to the time slot of data symbol. The Wiener filter can also be employed here to get a better channel estimation of training symbol.

### 3.3.3 Analysis of channel estimation error of polynomial interpolation



The channel estimation error at  $t$  th time slot and  $l$  th propagation path is

$$e(t, l) = h(t, l) - \hat{h}_{poly}(t, l) \quad (3.36)$$

The MSE of  $e(t, l)$  is obtained as follows

$$\begin{aligned} mse(t, l) &= E\{e(t, l)e^*(t, l)\} \\ &= E\{[h(t, l) - \hat{h}_{poly}(t, l)][h^*(t, l) - \hat{h}_{poly}^*(t, l)]\} \\ &= r_{TT,l}(0) - 2 \operatorname{Re}[\mathbf{a}_q(t) \mathbf{A}_{T,q}^\perp E\{h^*(t, l) \mathbf{h}_T(l)\}] \\ &\quad + \mathbf{a}_q(t) \mathbf{A}_{T,q}^\perp \mathbf{R}_{TT,l} \mathbf{A}_{T,q}^{\perp T} \mathbf{a}_q^T(t) + \frac{\sigma_t^2}{|A|^2} \mathbf{a}_q(t) \mathbf{A}_{T,q}^\perp \mathbf{A}_{T,q}^{\perp T} \mathbf{a}_q^T(t) \end{aligned} \quad (3.37)$$

where  $\mathbf{R}_{TT,l}$  is the autocorrelation matrix of  $\mathbf{h}_T(l)$ , and

$$\begin{aligned} \mathbf{h}_T(l) &= [h(0, l), h(1, l), \dots, h(K-1, l), \\ &\quad h(Kr_t, l), h(Kr_t+1, l), \dots, h(Kr_t+K-1, l)]^T \end{aligned} \quad (3.38)$$

the autocorrelation matrix  $\mathbf{R}_{TT,l} = E\{\mathbf{h}_T(l)\mathbf{h}_T^H(l)\}$ .  $r_{TT,l}(0)$  is diagonal element of  $\mathbf{R}_{TT,l}$ . The MSE are divided into two parts. The first parts are the first three terms in Eq. (3.37). They are called model errors, coming from the difference between polynomial model and real channel. We define the MSE of model error at  $t$ th time slot and  $l$ th propagation path as

$$\begin{aligned} mse_{model}(t,l) &= r_{TT,l}(0) - 2 \operatorname{Re}[\mathbf{a}_q(t)\mathbf{A}_{T,q}^\perp E\{h^*(t,l)\mathbf{h}_T(l)\}] \\ &\quad + \mathbf{a}_q(t)\mathbf{A}_{T,q}^\perp \mathbf{R}_{TT,l} \mathbf{A}_{T,q}^{\perp T} \mathbf{a}_q^T(t) \end{aligned} \quad (3.39)$$

The second part is the last term in Eq. (3.37). It is called noise error and comes from the deprecation of channel noise. We define the MSE of noise error at the  $t$ th time slot and  $l$ th propagation path as

$$mse_{noise}(t,l) = \frac{\sigma_t^2}{|A|^2} \mathbf{a}_q(t)\mathbf{A}_{T,q}^\perp \mathbf{A}_{T,q}^{\perp T} \mathbf{a}_q^T(t) \quad (3.40)$$

If we consider MSE of model error and noise error as a function of  $t$ . Both of the model error and the noise error increase when the interpolated channel time slot locates far from the training position. The averaging MSE over all data time slot is derived in order to observe the performance of polynomial interpolation for  $l$ th propagation path. The averaging MSE are also divided into the model error part and the noise error part. First of all, the averaging MSE of model error can be obtained by

$$\begin{aligned} MSE_{model}(l) &= \frac{1}{d} \sum_{t \in D} \{r_{TT,l}(0) - 2 \operatorname{Re}[\mathbf{a}_q(t)\mathbf{A}_{T,q}^\perp E\{h^*(t,l)\mathbf{h}_T(l)\}] \\ &\quad + \mathbf{a}_q(t)\mathbf{A}_{T,q}^\perp \mathbf{R}_{TT,l} \mathbf{A}_{T,q}^{\perp T} \mathbf{a}_q^T(t)\} \\ &= r_{TT,l}(0) - \frac{1}{d} \operatorname{Re}\{tr[\mathbf{A}_{D,q} \mathbf{A}_{T,q}^\perp (2\mathbf{R}_{TD,l} - \mathbf{R}_{TT,l} \mathbf{A}_{T,q}^\perp \mathbf{A}_{D,q}^T)]\} \end{aligned} \quad (3.41)$$

where  $d$  are total numbers of data time slot;  $\operatorname{Re}\{X\}$  is to catch real part of  $X$ ;  $tr[\mathbf{A}]$  is to get the trace of the matrix  $\mathbf{A}$ , and  $\mathbf{R}_{TD,l} = E\{\mathbf{h}_T(l)\mathbf{h}_D^H(l)\}$  is the cross correlation matrix between  $\mathbf{h}_T(l)$  and  $\mathbf{h}_D(l)$ .  $\mathbf{h}_D(l)$  is composed of  $l$ th

propagation path at data time slot. Because the second term in Eq. (3.41) increases with higher polynomial order, the averaging MSE decreases when the polynomial order gets higher. The smaller training rate makes larger averaging MSE. Because the smaller training rate has a longer time duration, it causes a larger difference between polynomial model and real channel tap. The higher polynomial order can be used to solve this problem. The elements of the autocorrelation matrix  $\mathbf{R}_{TT,l}$  and cross-correlation matrix  $\mathbf{R}_{TD,l}$  can be obtained in Eq. (3.5a). The Eq. (3.5a) contains the parameters of the discrete Doppler frequency. The higher Doppler frequency makes channel change more rapidly. In the case of high Doppler frequency, we can also use higher polynomial order to get an accurate model of time varying channel tap. The second part of averaging MSE is to average noise error. The averaging MSE of model error can be obtained by

$$\begin{aligned}
 MSE_{noise}(l) &= \frac{1}{d} \sum_{t \in D} \frac{\sigma_t^2}{|A|^2} \mathbf{a}_q(t) \mathbf{A}_{T,q}^\perp \mathbf{A}_{T,q}^{\perp T} \mathbf{a}_q^T(t) \\
 &= \frac{\sigma_t^2}{d|A|^2} \text{tr}[\mathbf{A}_{D,q} \mathbf{A}_{T,q}^\perp \mathbf{A}_{T,q}^{\perp T} \mathbf{A}_{D,q}^T]
 \end{aligned} \tag{3.42}$$

The noise error is independent of channel properties (i.e., the Doppler frequency and channel power profile). It is only relative to the training and data arrangement and the polynomial order. The averaging MSE of noise error becomes large when polynomial order is high. This result is opposite to the averaging MSE of model error. The model error is independent of SNR. The noise error dominates both MSE and BER performance in the low SNR environment. The model error dominates MSE or BER performance in high SNR environment. And the model error will cause error floor in MSE curve and BER curve. If the taps are selected well (i.e., Correct number of taps and Correct delay position are used) by MST algorithm. The MSE performance of sub-symbol polynomial interpolation over all channel taps is

$$MSE_{poly} = \frac{1}{N} \sum_{l=0}^{L-1} MSE_{model}(l) + MSE_{noise}(l) \quad (3.43)$$

In the Section 4.4, we will simulate MSE performance in different parameters of the system. We also show the simulation result and Eq. (3.43).

## 3.4 Polynomial interpolation of channel in time-frequency domain

In this section, we introduce an existing time-frequency domain polynomial interpolation [14]. Compared to the sub-symbol polynomial interpolation with the time-frequency domain polynomial interpolation, the sub-symbol polynomial interpolation is operated on fast fading channel. Fast fading channel means that channel changes several times in a symbol duration. The time-frequency domain polynomial interpolation is operated on slow fading channel. Slow fading channel means that channel changes once a symbol duration.

### 3.4.1 Polynomial interpolation algorithm in time-frequency domain

In the receiving end, we gain the received baseband signal of  $k$  th tone in the  $m$  th symbol interval is obtained by

$$R(m, k) = H(m, k)X(m, k) + W(m, k) \quad (3.44)$$

where  $W(m, k) = W_I(m, k) + jW_Q(m, k)$  is a zero mean complex Gaussian random variable with variance  $\sigma_w^2$ . A common practice for estimating  $H(m, k)$  is to insert

pilot symbols at some predetermined location in the time-frequency plane (seen in Figure 3.4). The LS channel estimation at pilot location can be estimated by

$$\hat{H}_{LS}(m, k) = \frac{R(m, k)}{X(m, k)} = H(m, k) + \frac{W(m, k)}{X(m, k)} \quad (3.45)$$

where  $W(m, k)/X(m, k)$  is the error term, due to presence of Gaussian noise with variance  $\sigma_w^2 / E\{|X(m, k)|^2\}$ . In the time-frequency interpolation [14], we select an operation window in the time-frequency plane first, in which  $N_0 \times M_0$  pilots are distributed uniformly at every  $r_f$  tone and every  $r_t$  symbol (see Figure 3.1).

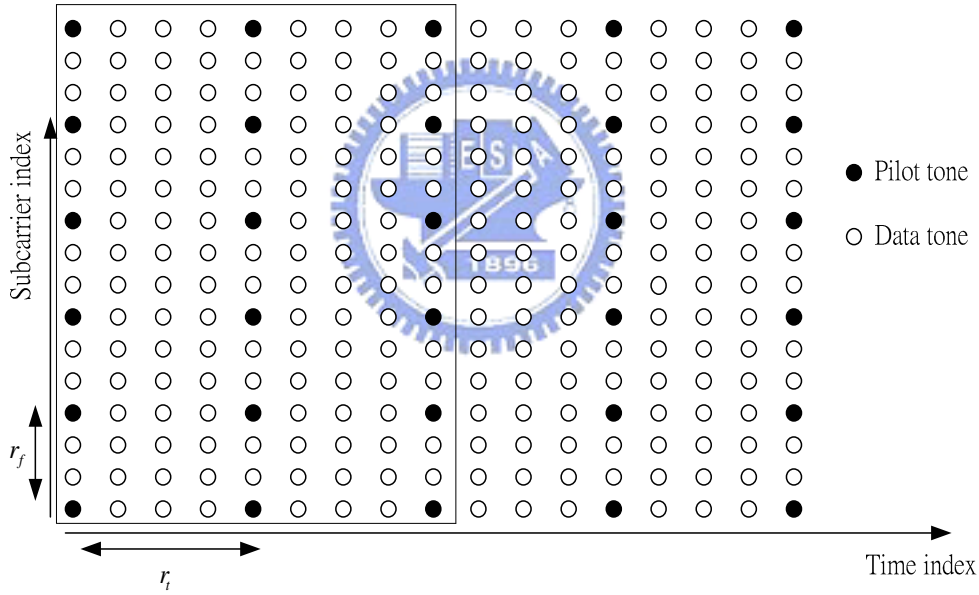


Fig. 3.4 Data grid in the time-frequency plane of OFDM signals

Then the receiver models the fading channel  $H_{mk}$  as a 2D (time-frequency) polynomial function

$$H_{poly}(m, k) = b_5 m^2 + b_4 m k + b_3 k^2 + b_2 m + b_1 k + b_0 \quad (3.46)$$

The frequency-domain model of the received samples implies that the ML estimates



of the coefficients  $[b_5, b_4, \dots, b_0] \equiv \mathbf{b}^T$  are chosen to satisfy the following criterion

$$\text{Min}_{\mathbf{b}} \sum_{(m,k) \in P} |R(m,k) - \mathbf{a}(m,k)\hat{\mathbf{b}}|^2 \quad (3.46)$$

where the set  $P$  in Eq. (3.20) contains the pilot locations in the operating window,

$$P = \left\{ (m,k) \left| \begin{array}{l} m = 0, r_f, \dots, (M_0 - 1)r_f \\ k = 0, r_t, \dots, (N_0 - 1)r_t \end{array} \right. \right\} \quad (3.47)$$

and  $\mathbf{a}(m,k) = [m^2, mk, k^2, m, k, 1]$  is called time-frequency vector, The polynomial coefficients for the time-frequency window can be shown as

$$\hat{\mathbf{b}} = \mathbf{A}_{t-f,T}^\perp \hat{\mathbf{H}}_{LS} \quad (3.48)$$

where  $\mathbf{A}_{t-f,T}$  is called training time-frequency matrix; every row of  $\mathbf{A}_{t-f,T}$  is the time-frequency vector corresponding the pilot location in the time-frequency window.

$\mathbf{A}_{t-f,T}^\perp$  is the pseudo inverse of  $\mathbf{A}_{t-f,T}$ . The channel interpolation of data location can be achieved by

$$\hat{H}_{poly}(m,k) = \mathbf{a}(m,k)\hat{\mathbf{b}}, \quad m,k \in D \quad (3.49)$$

where the set  $D$  contains locations of data symbol in the time-frequency window. A more complicated method that is capable of reducing the effect of noise is the LMMSE method. This method based on the estimated channel autocorrelation matrix and noise variance  $\sigma_f^2$  estimates channel frequency response on the pilot location which is shown as

$$\hat{\mathbf{H}}_{mmse} = \tilde{\mathbf{R}}_H [\tilde{\mathbf{R}}_H + \sigma_f^2 (\mathbf{X}\mathbf{X}^H)^{-1}]^{-1} \hat{\mathbf{H}}_{LS} \quad (3.50)$$

where  $\tilde{\mathbf{R}}_H$  is the channel autocorrelation function of pilot tones.  $\mathbf{X}$  is a diagonal matrix whose diagonal elements are the pilot amplitude. The  $\hat{\mathbf{H}}_{mmse}$  is substituted with  $\hat{\mathbf{H}}_{LS}$  in Eq. (3.24). Then the coefficients vector can be obtained by

$$\hat{\mathbf{b}}_{mmse} = \mathbf{A}_{t-f,T}^\perp \hat{\mathbf{H}}_{mmse} \quad (3.51)$$

Furthermore, the channel interpolation by Wiener filter smoothing and polynomial interpolation are obtained by

$$\hat{h}_{mmse}(m, k) = \mathbf{a}(m, k) \hat{\mathbf{b}}_{mmse} \quad (3.52)$$

In next paragraph, we will compare performance of sub-symbol polynomial interpolation with performance with the time-frequency domain polynomial interpolation.

### 3.4.2 The comparison between sub-symbol interpolation and time-frequency domain interpolation

The time-frequency domain interpolation use pilot tones for channel estimation in frequency domain. The other tones on the data location can be sent data. The sub-symbol polynomial interpolation uses training symbol for channel estimation in the time domain. It means all tones are pilot tones in an OFDM symbol. The pilot tones of time-frequency domain interpolation are distributed more uniformly than sub-symbol polynomial interpolation. The time-frequency polynomial interpolation seems have better performance than sub-symbol polynomial interpolation. But the variation of channel in the frequency domain is rapider than the variation of channel in the time domain (seen in Figurer 3.5). We will suffer a large model error when interpolate channel in frequency domain. In the simulation results, we will find that the performance of sub-symbol polynomial interpolation is better than the performance of time-frequency domain polynomial interpolation, due to rapid variation of channel in the frequency domain. In mobile channel assumption, the

sub-symbol polynomial interpolation assumes that channel changes several times in an OFDM symbol. We define this assumption as fast fading channel. The time-frequency assumes that channel doesn't change in an OFDM symbol and changes for different OFDM symbols. We define this assumption as slow fading channel. The sub-symbol polynomial interpolation is a channel estimation method based on fast fading channel. It is more general assumption of channel.

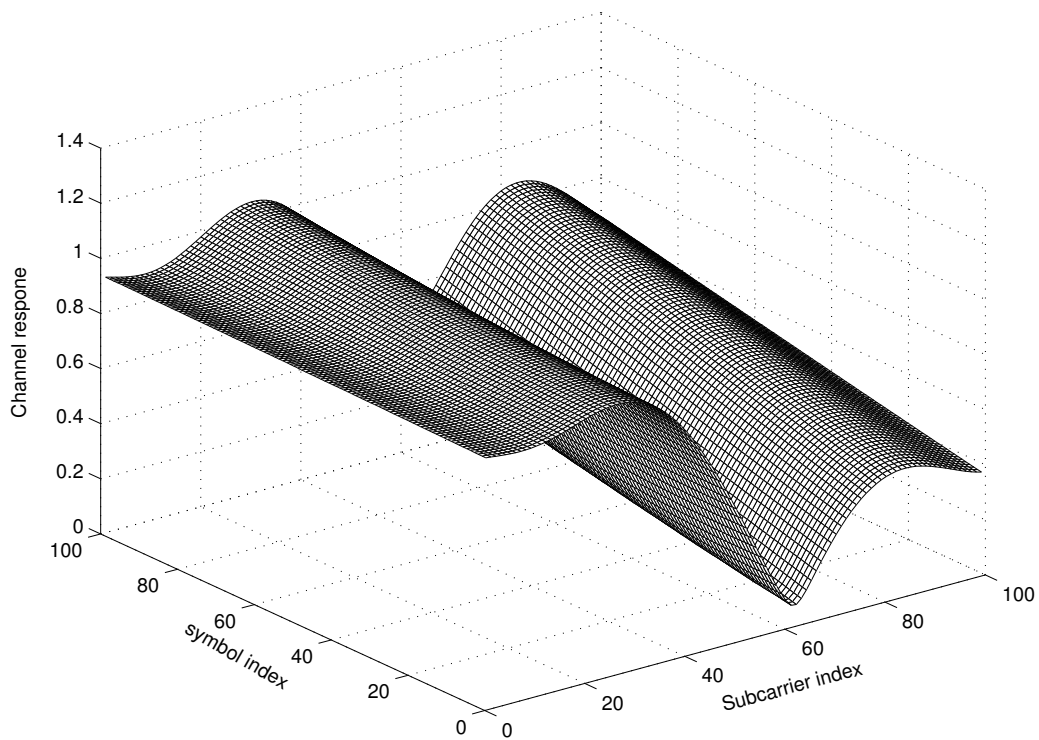


Fig. 3.5 Channel responses distribute in time-frequency plane.

# Chapter 4

## Computer Simulations

### 4.1 Simulation parameters

The channel model is evaluated by computer simulation for two multipath fading channel models, namely TI (time invariant) Channel-A and TI (time invariant) Channel-B, The TI Channel-A is the ATTC (Advanced Television Technology Center) and the Grand Alliance DTV laboratory's ensemble E model whose channel impulse response for the static case is given by

$$h[n] = \delta[n] + 0.3162\delta[n-2] + 0.1995\delta[n-17] + 0.1296\delta[n-36] + 0.1\delta[n-75] + 0.1\delta[n-137] \quad (4.1)$$

where unit delay is assumed to be the same as OFDM sample period. The TI Channel-B is a simplified version of DVB-T channel model  $P_1$  [23] and its channel impulse response for the static case is given by

$$h[n] = 0.2478\delta[n] + 0.1287\delta[n-1] + 0.3088\delta[n-3] + 0.4252\delta[n-4] + 0.49\delta[n-5] + 0.0365\delta[n-7] + 0.1197\delta[n-8] + 0.1948\delta[n-12] + 0.4189\delta[n-17] + 0.317\delta[n-24] + 0.2055\delta[n-29] + 0.1846\delta[n-49] \quad (4.2)$$

The time varying properties consult the DGUS channel model which is introduced in Section 3.1. The TI Channel-A can be modified to time varying model and is

represented as

$$h[n, t] = \mu_0(t)\delta[n] + 0.3162\mu_1(t)\delta[n - 2] + 0.1995\mu_2(t)\delta[n - 17] \\ + 0.1296\mu_3(t)\delta[n - 36] + 0.1\mu_4(t)\delta[n - 75] + 0.1\mu_5(t)\delta[n - 137] \quad (4.3)$$

This time varying channel model is called TV (time varying) Channel-A. Every complex Gaussian random process  $\mu_i(t)$  is composed of five complex sinusoid functions ( $N_i = 12$ ). There are six taps and every tap is composed of five complex sinusoid functions in the TV Channel-A. Therefore there are total thirty complex sinusoid functions to be used in the TV Channel-A. If the Doppler frequency is assigned to  $f_d$ , the frequencies of these sinusoid functions are distributed uniformly from 0 to  $f_d$ . The phase of these complex sinusoid functions are uniform distribution from 0 to  $2\pi$ . According to modification of TI Channel-A, the time varying model of TI Channel-B also can be created, and we call this time varying channel as TV (time varying) Channel-B. There are twelve taps in the TV Channel-B and every tap is composed of five complex sinusoid functions. Total sixty complex sinusoid functions is used in the TV Channel-B. If the Doppler shift is assigned to  $f_d$ , the frequencies of these sinusoid functions are distributed uniformly from 0 to  $f_d$ . The phase of these complex sinusoid functions are uniform distribution from 0 to  $2\pi$ . In OFDM system, The DVB [23] system is used in this chapter, for a 8MHz channels, the number of subcarriers  $N = 2048$  (2K mode), and guard interval ratio=1/8, the sampling rate are 10MHz and carrier modulation 64-QAM are used. The 64-QAM signal power is set to 1. In all methods, pilot tone symbol of  $1.0801 + j1.0801$  signal point in 64-QAM constellations is used.

## 4.2 Comparison between FPTA, MST and LMMSE in time invariant channel

In this section, we first observe the characteristics of FPTA, MST and LMMSE. Those characteristics are similar to the characteristics of modified methods which are used for time varying channel. In LMMSE method, ideal correlation and SNR values are used in order to evaluate the relative performance of MST method. Figure 4.1 shows the MSE performances of different channel estimation method and MSE of MST with 5 taps based on Eq. (2.26) in the TI Channel-A. The method of LMMSE has the same performance of MST with 6 taps, MST with 6 taps, which is the same as the number of taps in Channel-A, has approximately 18 to 22 dB MSE gain over FPTA. MST with 5 taps shows an irreducible channel estimation floor caused by missing some of the channel energy. The missing energy is shown in the first term of Eq. (2.26). In Eq. (2.26), we can find the error floor equal to missing tap energy. The energy of weakest tap in the TI Channel-A is -20dB and is the error floor of MSE in Figure 4.1. MST with 5 taps has a better performance than FPTA for SNR less than 20dB since for this SNR region the gain in noise suppression is greater than the loss of channel energy missing. However, for higher SNR region where noise has smaller impact than the channel energy missing, the error floor of channel estimation results in a worse performance for MST with 5 taps. In Figure 4.2, the BER performances in TI Channel-A are presented for the different channel estimation methods. Due to the channel estimation error floor and the sensitivity of 64-QAM to channel estimation error, MST with 5 taps case shows a BER floor while the others do not. Another most significant selection is the threshold decision. The suitable choice of threshold

depends on the operating SNR. The threshold is inverse proportion to multiple of SNR. Figure 4.3 shows several multiples of inversion of SNR in MSE performance. If the multiple is close to 1, missing taps will occur. If the multiple is too low, more noise will be injected. A proper multiple is 0.01 which can be shown in Figure 4.3. Figure 4.4 shows the BER performance in different multiples of inversion of SNR. Because large number of subcarriers is used in DVB system and construction of training symbol, most tones are set to zeros in training symbol. There are few taps in the channel models. In the receiver side, the received training signal, convolution of channel and training symbol adds noise, has many pure noise samples. If we ignore several powerful samples, we will get those pure noise samples. After averaging those pure noise samples, noise power can be estimated. Because the power of 64-QAM signal is set to 1, the SNR can be acquired by inverse of estimated noise power.

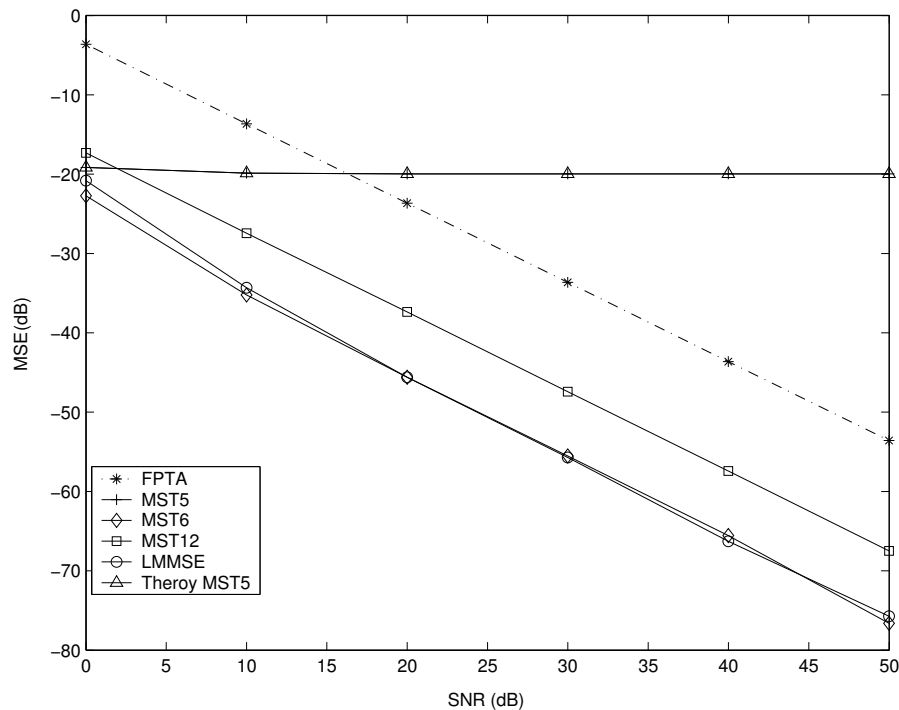


Fig. 4.1 Channel estimation mean square error (MSE) in TI Channel-A

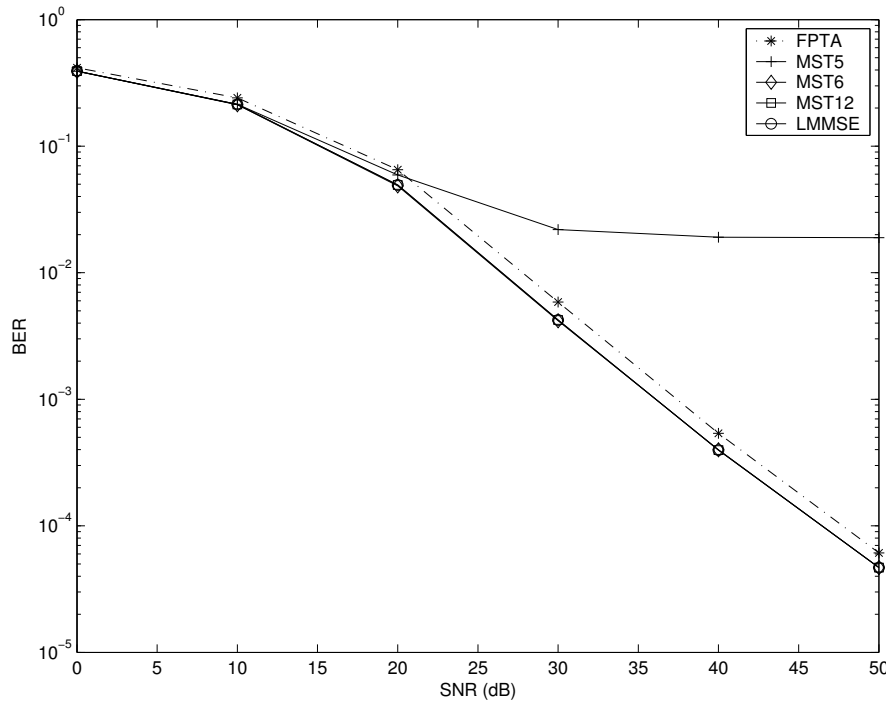


Fig. 4.2 BER performance with different channel estimation methods in TI

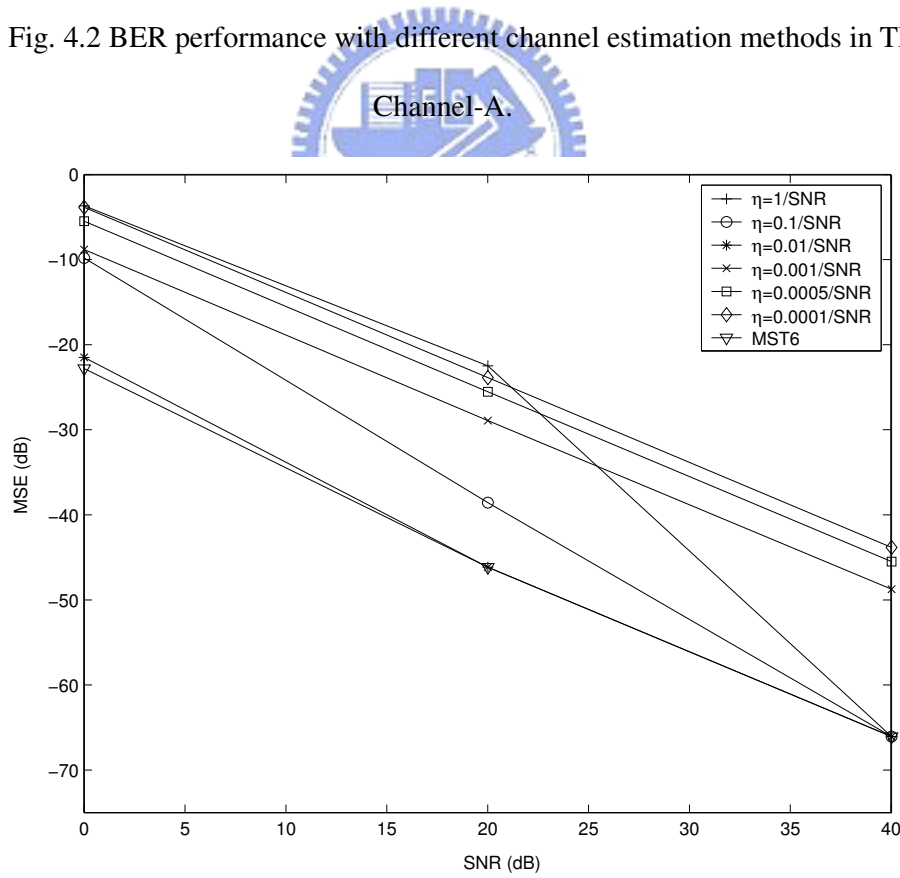


Fig. 4.3 Channel estimation MSE performance with different threshold selections in

TI Channel-A



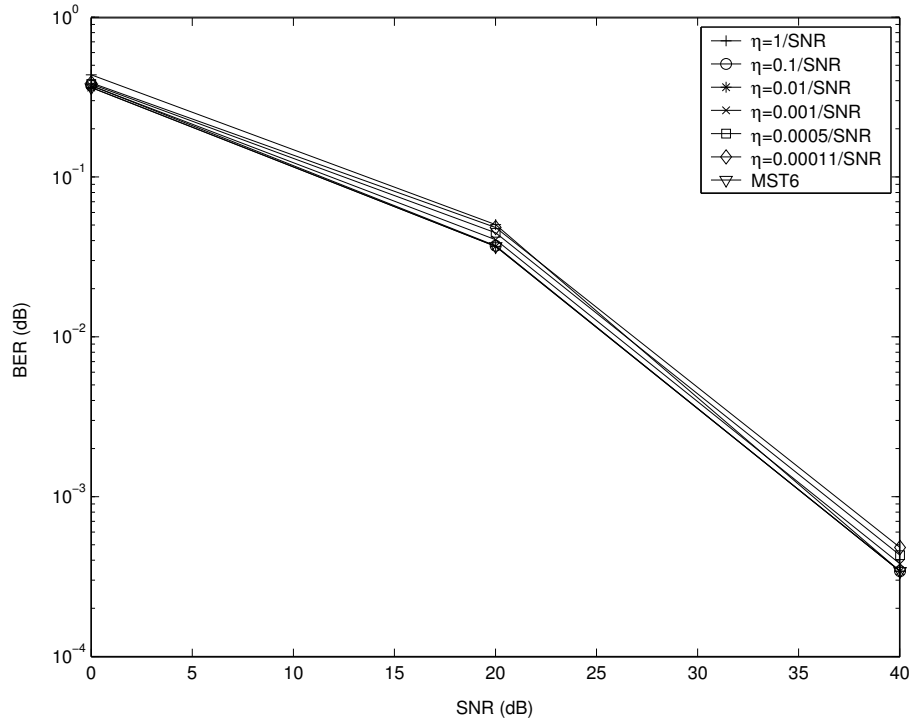


Fig. 4.4 BER performance with different threshold selections in TI Channel-A

### 4.3 Comparison between estimation methods in time varying channel

In this section, performance of channel estimation method in Chapter 3 will be shown in MSE and BER curves. The time varying channel model is represented in Section 4.1. TV Channel-A is used in Figure 4.5. Figure 4.5 shows the BER performance of FPTA with linear interpolation, MST with linear interpolation, FPTA with decision direct algorithm, MST with decision direct algorithm, the time-frequency domain polynomial interpolation and the sub-symbol polynomial interpolation with MST algorithm. The selection of taps in MST is 6 in this simulation. The performances of sub-symbol polynomial interpolations are better than linear

interpolations due to smaller model error. If total numbers of pilot tones are the same, the pilot tones distribute more uniformly than training symbol in time-frequency domain than in sub-symbol methods. Therefore performance of time-frequency domain polynomial interpolation seems better than sub-symbol polynomial interpolation. Due to the variation of channel in frequency domain is rapider than the variation of channel in time domain, the time-frequency domain polynomial interpolation is worse than sub-symbol polynomial interpolation. Time-frequency domain polynomial interpolation is more complex than sub-symbol polynomial interpolation. The decision direct algorithm may cause error propagation. Performance of decision direct algorithm is worse than polynomial interpolations and linear interpolation due to error propagation.

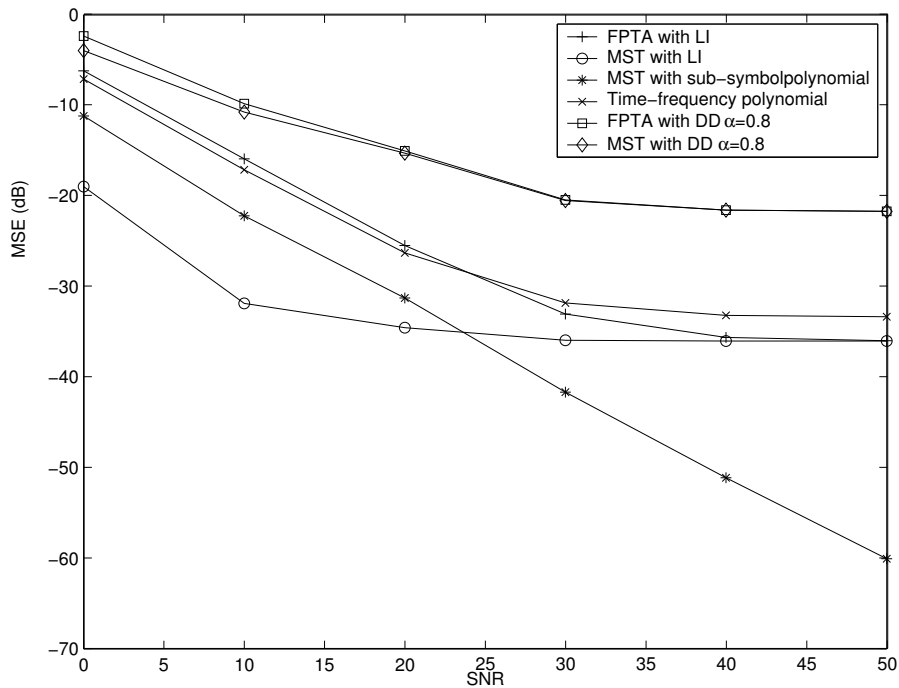


Fig. 4.5 MSE performance with different channel estimation methods in Doppler frequency 75Hz environment.

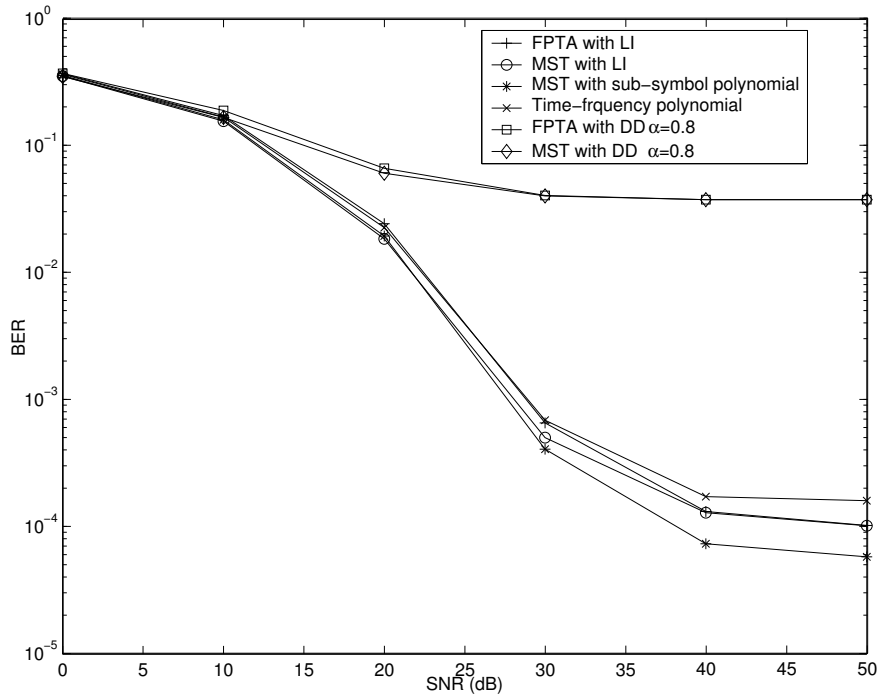


Fig. 4.6 BER performance with different channel estimation methods in Doppler frequency 75Hz environment.

Figure 4.7 shows the different selection of taps in MST combining sub-symbol polynomial interpolation in the Doppler frequency 75Hz. The result shows that the suitable threshold value is -20dB below inverse of SNR. MST with 5 taps also cause error floor in sub-symbol polynomial interpolation with MST method. The error floor in other methods comes from Doppler effects.

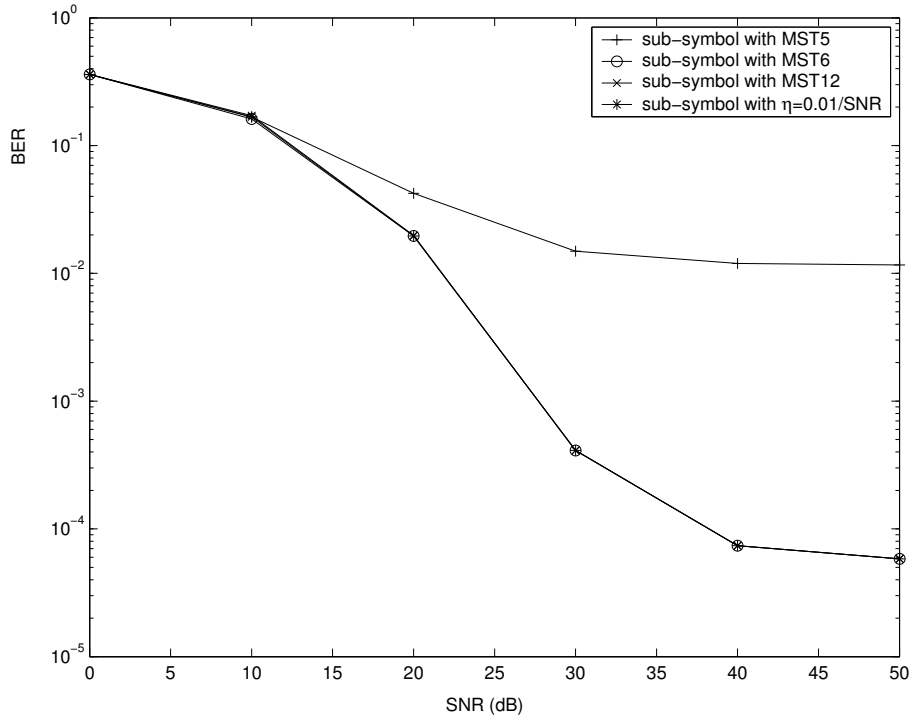


Fig. 4.7 BER performance with different taps selection of Combining MST and sub-symbol polynomial interpolation.

## 4.4 Properties of sub-symbol polynomial interpolation

The MSE performance of the sub-symbol polynomial interpolation is derived in Section 3.4. The MSE is divided into the model error and the noise error. Both of the model error and noise error are sensitive to several parameters of the OFDM system. In this section, we observe sensitivity of the model error and sensitivity of the noise error in differential parameters of OFDM system. These parameters include Doppler frequency, training rate, polynomial order and different channel statistics (TV Channel-A and TV Channel-B). The MST algorithm combines with time domain

polynomial interpolation, is used in the simulations of this section. When the channel environment is TV Channel-A, we do MST with six taps, and the time domain polynomial interpolation interpolates these six taps. MST with twelve taps is adopted in TV Channel-B environment. Then we do the sub-symbol polynomial interpolation for these twelve taps. In the simulation result, the performance of MSE has a little poor compared to theory value of MSE.

#### 4.4.1 Comparison of different Doppler frequency

In this paragraph, MSE performance of channel estimation is discussed with different Doppler frequencies. We fix the training rate with 1/8. The polynomial order is set to two, and TV Channel-A is used. The MSE performances with different Doppler frequencies (90Hz, 100Hz, 150Hz) are observed in Figure 4.8.

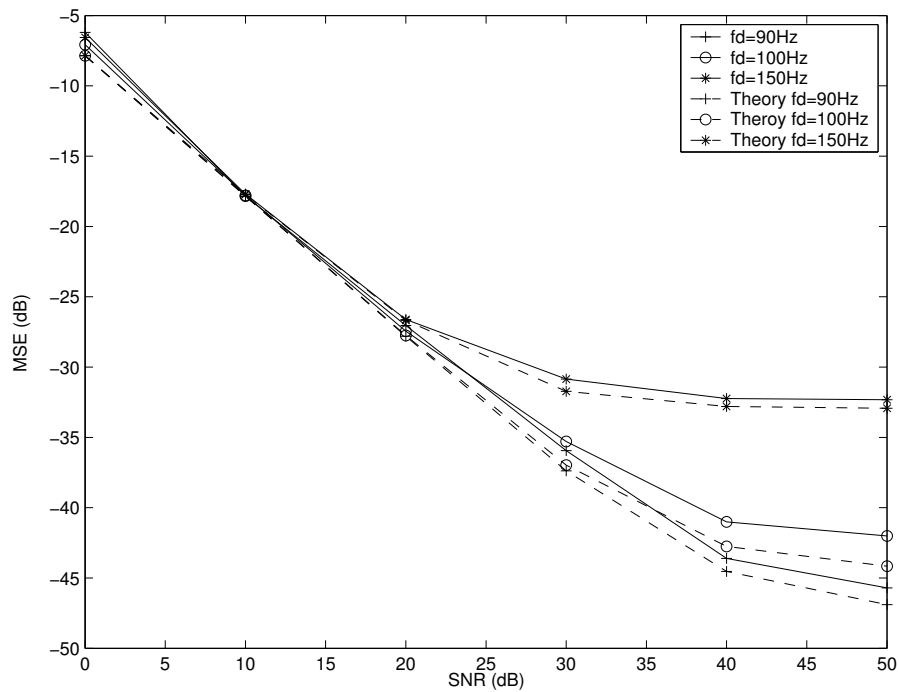


Fig. 4.8 Channel estimation MSE with different Doppler frequencies in TV Channel-A

Figure 4.8 is divided into two parts in order to distinguish the model error and noise error. The first part is low SNR region. The noise error dominates MSE performance in this region. The second part is high SNR region. The model error dominates MSE performance in this region. The three curves overlap in low SNR region. It means that the noise error is independent of the Doppler frequency. In high SNR region, the MSE curves have error floor. This error floor is the model error. We can see clearly in Figure 4.8, the higher Doppler frequency curve has the higher model error. This problem of model error can be solved by increasing polynomial order or decreasing training rate. We will discuss properties of these two solutions in next two paragraphs.

#### **4.4.2 Comparison of different training rate**

In this paragraph, we will show how the training rate affects the MSE performance of channel estimation. The Doppler frequency is fixed to 150Hz. Polynomial order is set to two, and TV Channel-A is used. The MSE performances with different training rates (1/4, 1/8) are observed in Figure 4.9.

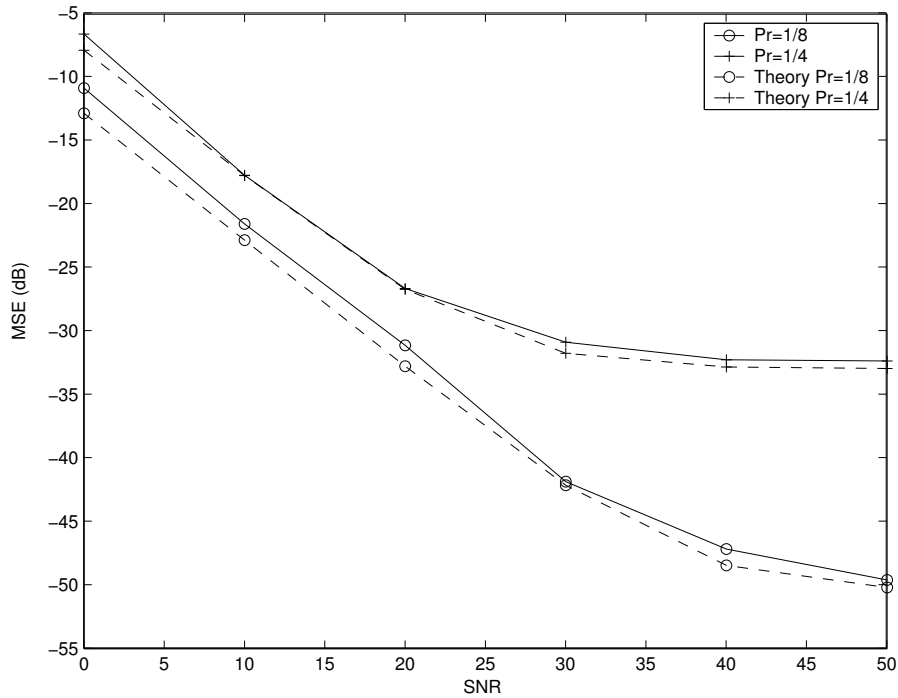


Fig. 4.9 Channel estimation MSE with different training rates in TV Channel-A

Figure 4.9 is also divided into two parts in order to distinguish the property of model error and property of noise error. The first part is low SNR region. The noise error dominates MSE performance in this region. The second part is high SNR section. The model error dominates MSE performance in this section. The larger training rate has lower noise error in low SNR section. It means that the noise error increases when training rate increases. The MSE curves have error floor, this error floor is the model error. We can see clearly in Figure 4.9, the large training rate curve also has low model error.

### 4.4.3 Comparison of different polynomial order

The polynomial order is parameter which affects MSE performance. The effect of

polynomial order is debated in this paragraph. First we fix the training rate to 1/8, the Doppler frequency is 200Hz, and TV Channel-A is used. The MSE performances with different polynomial order (2, 3, 4, 5) are observed in Figure 4.12.

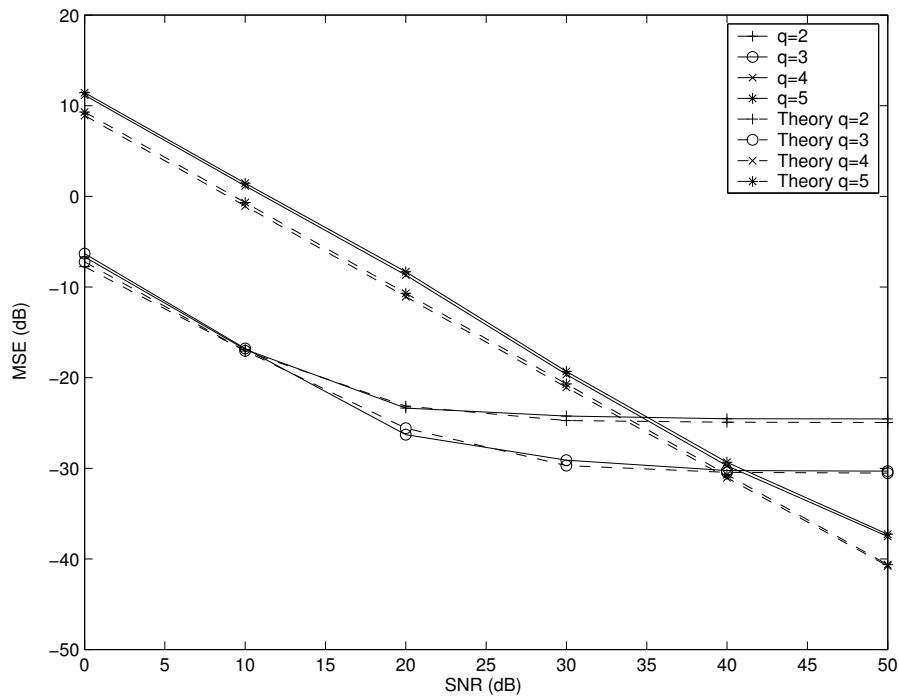


Fig. 4.10 Channel estimation MSE with different polynomial order in TV Channel-A

Figure 4.10 is also divided into two parts in order to distinguish the model error and noise error. The first part is low SNR section. The noise error dominates MSE performance in this section. The second part is high SNR section. The model error dominates MSE performance in this section. The higher polynomial order curve has the higher noise error in low SNR section. It means that the noise error increase when polynomial order is high. In high SNR section, the MSE curves have error floor. This error floor is the model error. We can see in Figure 4.10, the higher polynomial order curve has lower model error. There is a tradeoff between noise error and model error in choosing polynomial order.



#### 4.4.4 Comparison of different channel model

In this paragraph, the different channel model is discussed in MSE performance. We fix the training rate as 1/4; the Doppler frequency as 100Hz and 150Hz. Polynomial order is set to two. The MSE performances with different channel model (TV Channel-A and TV Channel-B) are observed in Figure 4.11.

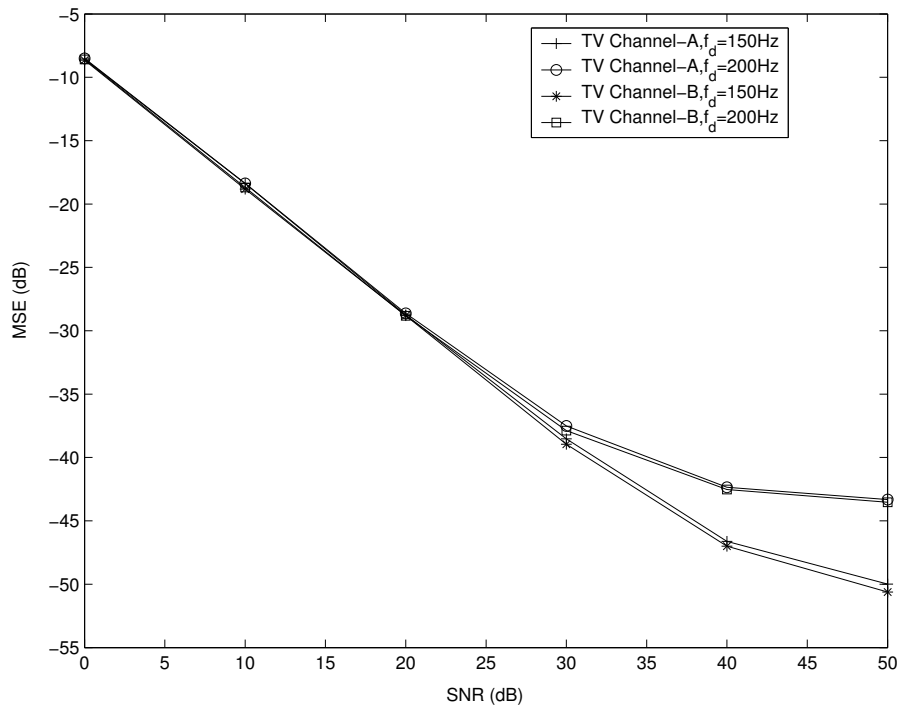


Fig. 4.11 Channel estimation MSE in TV Channel-A and TV Channel-B and  $f_d =$   
150Hz, 200Hz.

The TV Channel-A has the same delay spread with the TV Channel-B. Figure 4.11 is also divided into two parts in order to distinguish the model error and noise error. The first part is low SNR region. The noise error dominates MSE performance in this

section. The second part is high SNR region. The model error dominates MSE performance in this region. The noise error is independent of Doppler frequency and channel model, because these curves overlap in the low SNR region. In high SNR region, the MSE curves have error floor. This error floor is the model error. The model errors in the same Doppler frequency have a little difference between two channel models. MSE performance of TV channel B is a little better than MSE performance of TV Channel A.

We observe sensitivity of the model error and noise error in this section. Then we find that noise error is nonsensitive totally to the channel condition. The noise error is only sensitive to training rate and polynomial order. The model error is sensitive to all parameters observed in this section. In the low SNR region, the noise error dominates the MSE performance. Since the noise error is not sensitive to channel, we can say the sub-symbol polynomial interpolation is robust channel estimation method in the low SNR region. But the width of low SNR region is relative to the model error. In bad channel condition, large Doppler frequency, the model error may be large and cause error floor from a low SNR value.

# Chapter 5

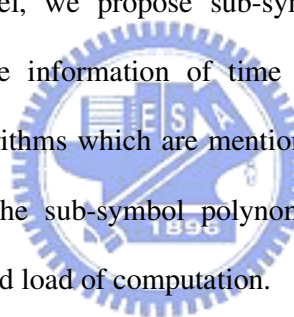
## Conclusion

Channel estimation of time varying channel is a challenge because of tracking channel variation. We introduce several interpolation techniques to track channel variation. The FPTA or MST with decision directed algorithm is intolerable in simulation results because of large decision error. The linear interpolation is the simplest way to track channel variation, but the large model error will occur in high Doppler frequency environment and low training rate system. In high Doppler shift, variation of channel is more like a polynomial function whose order is more than one. Low training rate system has a long duration between two training symbol. Linear approach of channel is not suitable for this long duration. In fast fading channel, we propose the sub-symbol polynomial interpolation, together with the MST algorithm to reduce the model error of linear interpolation. We analyze the MSE of sub-symbol polynomial interpolation, and the MSE is divided into two parts. One is the noise error, the other is the model error. For the noise error, we find that it is independent of the Doppler frequency and other statistics of channel. The noise error depends on training rate and polynomial order. The performance of the noise error becomes worse

by decreasing training rate and increasing polynomial order. The model error is sensitive to the Doppler frequency, statistics of channel, training rate and polynomial order. The model error becomes worse by increasing Doppler frequency, decreasing training rate and decreasing polynomial order.

The MST algorithm can be used in sub-symbol polynomial interpolation. There are two advantages of most significant taps selection. It reduces the computation and suppresses noise. But the MST method has a problem of missing taps. The error floor of MSE will appear when missing taps occurs. In the Chapter 2, we also analyze MSE of MST method under missing taps. The results of analysis reveal that the error floor is equal to the power of missed taps.

In the fast fading channel, we propose sub-symbol polynomial interpolation. Because it can collect more information of time varying channel, it has better performance than other algorithms which are mentioned before. Combing with most significant taps algorithm, the sub-symbol polynomial interpolation will perform better in noise suppression and load of computation.



# Bibliography

- [1] R. W. Chang, "Synthesis of band-limited orthogonal signals for multi-channel data transmission," *Bell Syst Tec. Journal*, vol. 45, Dec. 1966.
- [2] L. J. Cimini, Jr., "Analysis and simulation of a digital mobile channel using orthogonal frequency-division multiplexing," *IEEE Trans. Comun.*, vol. 33, no.7, pp. 665-675, July 1985.
- [3] J.A. C. Bingham, "Muticarrier modulation for data transmission: An idea whose time has come," *IEEE Trans. Comun. Mag.*, vol. 28, no. 5, pp. 5-14, May 1990.
- [4] *Asymmetric digital subscriber line(ADSL) metallic interface*, American National Standard Institute (ANSI), Dec. 1995.
- [5] P. Shelswell, "The COFDM modulation system: The heart of digital audio broadcasting ," *Elec. Commun. Eng. Journal*, pp. 127-136, June 1995.
- [6] U. Reimers, "Digital vedio broadcast," *IEEE Communications Mag*, vol. 36, no. 6, pp. 104-110, June 1998.
- [7] R. van Nee and G. Awater, "New high-rate wireless LAN standards," *IEEE Communications Magzine*, pp.82-88, Dec. 1999.
- [8] Xiaobo Zhou and Xiaodong Wang., " Channel estimation for OFDM systems using adaptive radial basis function networks," *IEEE Trans. Vehic*, vol. 52, pp. 48-59, Jan 2003
- [9] K. S. Gilhousen et al., "On the capacity of a cellular CDMA system", *IEEE Trans. Vehic. Technol*, vol. 40, pp. 303-312. May 1991.
- [10] H. W. Li and J. K. Cavers, "An adaptive filtering technique for pilot-aided

transmission systems,” *IEEE Trans. Vehic Technol*, vol. 40, pp. 532-545 Aug 1991

- [11] Ye Li, “Pilot-symbol-aided channel estimation for OFDM in wireless systems,” *IEEE Trans. Commun.*, vol. 49, NO. 4, pp. 1207-1215 July 2000.
- [12] C. D’Amours, M. Moher, and A. Yongaçoğlu, “Comparison of pilot symbol-assisted and differentially detected BPSK for DS-CDMA systems employing RAKE receivers in Rayleigh fading channels, *IEEE Trans. Vehic. Technol.*, vol. 47 pp. 1258-1267, Nov 1998.
- [13] C. S. Yeh, Y. Lin, and Yiyan Wu, “OFDM system channel estimation using time-domain training sequence for mobile reception of digital terrestrial broadcasting,” *IEEE Trans. Broad. Vol.* 46, pp. 215-219, Sept 2000.
- [14] M. X. Chang and Tu T. Su, “Model-based channel estimation for OFDM signal in Rayleigh fading,” *IEEE Trans. Commun.*, vol. 50, pp. 540-544, April 2002.
- [15] Xiaowen Wang, “Channel estimation for multicarrier modulation systems using a time-frequency polynomial model,” *IEEE Trans. Commun.*, vol. 7, pp. 1045-1048, July 2002
- [16] Deva K. Borah and Brian D. Hart, “Frequency-selective fading channel estimation with a polynomial time-varying channel model,” *IEEE Trans. Commun.*, Vol. 47, pp. 862-873, June 1999.
- [17] Hlaing Minn and Vijay K. Bhargava, “An Investigation into Time Domain Approach for OFDM channel Estimation,” *IEEE Trans. Commun.*, vol. 46, pp. 240-248, December 2000.
- [18] Ove Edfors and M. Sandell, “OFDM channel estimation by singular value decomposition,” *IEEE Trans. Commun.*, vol. 46, July 1998.
- [19] Sarah Kate Wilson, Ellen Khayata and John M. Cioffi, “16 QAM modulation with orthogonal frequency division multiplexing in a Rayleigh-fading environment,” *In Proc. VTC 1994*, pp. 1660-1664, Stockholm, Sweden, June

1994.

- [20] Pätzold M., Killat U., Laue F., and Li Y., "On the statistical properties of deterministic simulation models for mobile fading channels," *IEEE Trans. Veh Technol.* vol. 1, pp. 254-269. 1998.
- [21] Pätzold M., "Mobile fading channels modeling, analysis, and simulation," Vieweg, widebaden, Germany. 1999.
- [22] Bello M., "Characterization of randomly time-variant linear channels," *IEEE Trans. Commun.*, vol. 4 pp. 360-393, 1963.
- [23] *Digital video broadcasting (DVB) : Framing, channel coding and modulation for digital terrestrial television*, Draft ETSI EN300 744 V1.3.1 (2000-08).

